

NATIONAL ADVISORY COMMITTEE FOR AERONAUTICS

TECHNICAL NOTE 2217

ANALYSIS OF PLANE-STRESS PROBLEMS WITH AXIAL
SYMMETRY IN STRAIN-HARDENING RANGE

By M. H. Lee Wu

Lewis Flight Propulsion Laboratory
Cleveland, Ohio

FOR REFERENCE

~~NOT TO BE TAKEN FROM THIS ROOM~~



Washington
December 1950

LIBRARY COPY

MAY 6 1953

LANGLEY RESEARCH CENTER
LIBRARY NASA
HAMPTON, VIRGINIA



3 1176 01433 9692

NATIONAL ADVISORY COMMITTEE FOR AERONAUTICS

TECHNICAL NOTE 2217

ANALYSIS OF PLANE-STRESS PROBLEMS WITH AXIAL

SYMMETRY IN STRAIN-HARDENING RANGE

By M. H. Lee Wu

SUMMARY

A simple method is developed to solve plane-stress problems with axial symmetry in the strain-hardening range based on the deformation theory of plasticity employing the finite-strain concept. The equations defining the problems are first reduced to two simultaneous nonlinear differential equations involving two dependent variables: (a) the octahedral shear strain, and (b) a parameter indicating the ratio of principal stresses. By multiplying the load and dividing the radius by an arbitrary constant, it is possible to solve these problems without iteration for any value of the modified load. The constant is determined later by the boundary condition.

The method is applied to the cases of a circular membrane under pressure, a rotating disk without and with a hole, and an infinite plate with a circular hole. Two materials, Inconel X and 16-25-6, the octahedral shear stress-strain relations of which do not follow the power law, are used. Distributions of octahedral shear strain, as well as of principal stresses and strains, are obtained. These results are compared with the results of the same problems in the elastic range. The variation of load with maximum octahedral shear strain of the member is also investigated.

The following results are obtained:

1. The ratios of the principal stresses remain essentially constant during loading and consequently the deformation theory is applicable to this group of problems.
2. In the plastic deformation, the distributions of the principal strains, and of the octahedral shear strain, are less uniform than in the elastic case, although the distributions of the principal stresses are more uniform. The stress concentration factor around the hole is reduced with plastic deformation, but a high strain concentration factor occurs.
3. The deformation that can be accepted by the member before failure depends mainly on the maximum octahedral shear strain of the material.

4. The added load that the member can sustain between the onset of yielding and failure depends mainly upon the octahedral shear stress-strain relation of the material.

INTRODUCTION

In the design of turbine rotors, it is desirable to know the detailed stress and strain distributions in the strain-hardening range and the amount of increase in load that can be sustained between the onset of yielding and failure. It is also desirable to know the effects of a notch or a hole in a turbine rotor or other machine members that are stressed in the strain-hardening range. If a member is thin, it can be analyzed on the basis of plane stress. For problems of this type, Nadai obtained solutions for ideally plastic material in the cases of the rotating disk, the thin plate with a hole, and the flat ring radially stressed (references 1 and 2). For the case of materials having strain-hardening characteristics, a solution of plane-stress problems has been obtained by Gleyzal for the circular membrane under pressure (reference 3). The concept of infinitesimal strain was used and the solution was obtained by an iterative procedure with a good first approximate solution. The plastic laws were always satisfied by using a chart given in reference 3. In reference 4, a trial-and-error method is given for rotating disk with very small plastic strain, in which the elastic stresses and strains are used as the first approximate values. Experimental investigation for the high-speed rotating disk is made in reference 5; distributions of plastic strains (logarithmic strains) for different types of disk are measured. Reference 6 experimentally investigates the burst characteristics of rotating disks; stress at the center of disk is calculated by assuming that the material behaves elastically at the burst speed; the average tangential stress along the radius at burst speed is also calculated.

A simple method of solving plane-plastic-stress problems with axial symmetry employing the finite strain concept in the strain-hardening range and based on the deformation theory of Hencky and Nadai (references 7 to 9), which is derived under the condition that the directions and the ratios of the principal stresses remain constant during loading, was developed at the NACA Lewis laboratory and is presented herein. The equations of equilibrium, strain, and plastic law are reduced to two simultaneous nonlinear differential equations involving three variables, one independent and two dependent, that can be integrated numerically to any desired accuracy. These variables are the proportionate radial distance, the octahedral shear strain, and a parameter α that indicates the ratio of principal stresses. The magnitude of variation in calculated values of the parameter α with change in load directly indicates whether the deformation theory is applicable to the problem.

The method developed is applied to: (1) a circular membrane under pressure, in order to compare results obtained by this method with that

obtained by Gleyzal (reference 3); (2) rotating disks without and with a circular central hole, in order to investigate plastic deformation in such disks and the effects of the hole; and (3) an infinite plate with a circular hole or a flat ring radially stressed, in order to investigate the effects of the hole in the strain-hardening range.

In the investigation of (2) and (3), two materials, Inconel X and 16-25-6, with different strain-hardening characteristics were used in order to determine the effect of the octahedral shear stress-strain curve on plastic deformation. The octahedral shear stress of these two materials is not a power function of the octahedral shear strain, so that more general information can be obtained. Distributions of stresses and strains of the same problems in the elastic range are also calculated for purposes of comparison.

SYMBOLS

The following symbols are used in this report:

- a radius of hole
- b outside radius of membrane, rotating disk, or flat ring
- c outside radius of plate, very large compared with radius a
- h instantaneous thickness of membrane, rotating disk, or plate
- h_i initial thickness
- k arbitrary constant
- p pressure on membrane
- r radial coordinate
- s arc length
- u radial displacement
- w axial displacement
- z axial coordinate
- α parameter indicating ratio of principal stresses
- γ octahedral shear strain
- ϵ logarithmic strain
- θ angular coordinate
- ρ mass per unit volume
- σ normal stress, normal force per unit instantaneous area

τ octahedral shear stress

ω angular velocity

Subscripts:

b at radius b

c at radius c

o at center, for case without hole or at radius a for case with concentric circular hole

1,2,3 principal directions in general

r, θ ,z principal directions in cylindrical coordinate system

STRESS-STRAIN RELATIONS IN PLASTIC DEFORMATION

The deformation theory of plasticity for ideally plastic materials was developed by Hencky from the theory of Saint Venant-Levy-Mises for the cases in which the directions and the ratios of principal stresses remain constant during loading (reference 7). Nadai extended the theory to include materials having strain-hardening characteristics (references 8 and 9). The conditions for the deformation theory have been emphasized by Nadai (reference 9, p. 209), Ilyushin (references 10 and 11), Prager (reference 12), and Drucker (reference 13). Experiments conducted by Lessells and MacGregor (reference 14), Osgood (reference 15), and others on thin tubes subjected to combined loads with the directions and the ratios of the principal stresses constant throughout the body and remaining constant during loading show that good results can be expected from the deformation theory.

In more recent experiments on thin tubes by Fraenkel (reference 16) and Davis and Parker (reference 17), it has been shown that even with considerable variation of the ratio of principal stresses during loading, the strains obtained from the experiments were in good agreement with the strains predicted by use of the deformation theory. Further experimental investigation is needed to determine the extent to which the variation of ratios of principal stresses is permissible. In case the variation is small (approximately 10 percent over the strain-hardening range), the deformation theory can, however, be expected to give good results.

In the present problems with axial symmetry, the directions of the axes of principal stress remain fixed during loading and it seems that the ratios of principal strains and of principal stresses may also remain approximately constant. The deformation theory previously discussed is therefore used. The stress-strain relations are then as follows:

$$\epsilon_1 + \epsilon_2 + \epsilon_3 = 0 \quad (1)$$

$$\frac{\sigma_1 - \sigma_2}{\epsilon_1 - \epsilon_2} = \frac{\sigma_2 - \sigma_3}{\epsilon_2 - \epsilon_3} = \frac{\sigma_3 - \sigma_1}{\epsilon_3 - \epsilon_1} \quad (2)$$

$$\tau = \tau(\gamma) \quad (3)$$

where

$$\tau = \frac{1}{3} \left[(\sigma_1 - \sigma_2)^2 + (\sigma_2 - \sigma_3)^2 + (\sigma_3 - \sigma_1)^2 \right]^{1/2} \quad (4a)$$

$$\gamma = \frac{2}{3} \left[(\epsilon_1 - \epsilon_2)^2 + (\epsilon_2 - \epsilon_3)^2 + (\epsilon_3 - \epsilon_1)^2 \right]^{1/2} \quad (4b)$$

From equations (1) to (4b), the following relations are obtained:

$$\epsilon_1 = \frac{1}{3} \frac{\gamma}{\tau} \left[\sigma_1 - \frac{1}{2} (\sigma_2 + \sigma_3) \right]$$

$$\epsilon_2 = \frac{1}{3} \frac{\gamma}{\tau} \left[\sigma_2 - \frac{1}{2} (\sigma_3 + \sigma_1) \right]$$

$$\epsilon_3 = \frac{1}{3} \frac{\gamma}{\tau} \left[\sigma_3 - \frac{1}{2} (\sigma_1 + \sigma_2) \right]$$

For plane-stress problems $\sigma_3 = 0$, so that

$$\tau = \frac{\sqrt{2}}{3} (\sigma_1^2 - \sigma_1 \sigma_2 + \sigma_2^2)^{1/2} \quad (5a)$$

$$\gamma = 2\sqrt{\frac{2}{3}} (\epsilon_1^2 + \epsilon_1 \epsilon_2 + \epsilon_2^2)^{1/2} \quad (5b)$$

and

$$\epsilon_1 = \frac{1}{3} \frac{\gamma}{\tau} (\sigma_1 - \frac{1}{2} \sigma_2) \quad (6a)$$

$$\epsilon_2 = \frac{1}{3} \frac{\gamma}{\tau} (\sigma_2 - \frac{1}{2} \sigma_1) \quad (6b)$$

$$\epsilon_3 = \frac{1}{3} \frac{\gamma}{\tau} \left[-\frac{1}{2} (\sigma_1 + \sigma_2) \right] = -(\epsilon_1 + \epsilon_2) \quad (6c)$$

When σ_1 and σ_2 are expressed in terms of ϵ_1 and ϵ_2 , there is obtained

$$\left. \begin{aligned} \sigma_1 &= 2 \frac{\tau}{\gamma} (2\epsilon_1 + \epsilon_2) \\ \sigma_2 &= 2 \frac{\tau}{\gamma} (2\epsilon_2 + \epsilon_1) \end{aligned} \right\} \quad (7)$$

EQUATIONS OF EQUILIBRIUM AND STRAIN INVOLVING DISPLACEMENTS

Equations of equilibrium and equations of strain are derived for three plane-stress problems with axial symmetry. It is convenient to use cylindrical coordinates for these derivations; the principle directions 1, 2, and 3 in the preceding equations become radial, circumferential, and axial directions, respectively. Because a large deformation in the strain-hardening range will be considered, the concept that the change of dimension of an element is infinitesimal compared with the original dimension of the element is not accurate enough. Hence, the finite-strain concept, which considers the instantaneous dimension of the element, is used. (The equations of infinitesimal strains will be given by considering them as special cases of finite strains.) The stress is then equal to the force divided by the instantaneous area and the strains are defined by the following equation:

$$\delta(\epsilon_j) = \frac{\delta(l_j)}{l_j}$$

where l_j is the instantaneous length of a small element having the original length of $(l_j)_0$ and $j = 1, 2$, and 3. During plastic deformation, the plastic strains at a certain state depend on the path

by which that state is reached. For the paths along which the ratios of principal stresses remain constant during loading, however, the octahedral shear stress-strain relation, the value of the octahedral shear strain, and the value of the principal strains are defined by the initial and final states (reference 15 and reference 9, p. 209); $\delta(\epsilon_j)$ is then an exact differential and

$$\epsilon_j = \log_e \frac{l_j}{(l_j)_0} \quad (8)$$

It should be noted that the condition under which equation (8) was obtained is also one of the conditions under which the deformation theory is derived; as long as the deformation theory is applicable, equation (8) can also be used.

Circular Membrane under Pressure

The membrane considered is so thin that bending stress can be neglected (reference 18, p. 576). Figure 1 shows the membrane clamped at the rim and subjected to a pressure p , and a small element defined by $\Delta\theta$ and Δs taken at radius $r+u$ in the deformed state. In the undeformed state, the same element would be at radius r and defined by $\Delta\theta$ and Δr . The instantaneous thickness of the element and the stresses acting on the element are also shown in the figure. The two principal stresses are σ_r and σ_θ , and φ is the angle between σ_r and the original radial direction.

Equations of equilibrium. - When all the forces acting on the element in the direction of σ_r are summed up, the following equation of equilibrium is obtained:

$$\begin{aligned} \sigma_r (r+u) h \Delta\theta - (\sigma_r + \Delta\sigma_r) [r+u + \Delta(r+u)] \Delta\theta (h + \Delta h) \cos \Delta\varphi + \\ 2\sigma_\theta \Delta s (h + \frac{1}{2} \Delta h) \sin \frac{\Delta\theta}{2} \cos \varphi - p \Delta s (r+u) \Delta\theta \sin \frac{\Delta\varphi}{2} \\ = 0 \end{aligned}$$

When $\Delta(r+u)$ approaches zero as a limit, the differential equation of equilibrium may be obtained:

$$(r+u) \frac{d(\sigma_r h)}{d(r+u)} = h(\sigma_\theta - \sigma_r) \quad (9)$$

A cap of the membrane bounded by radius $r+u$ and the forces acting on it are shown in figure 2. Summing up the forces in the z -direction yields

$$p\pi (r+u)^2 = \sigma_r \frac{dw}{ds} 2\pi h(r+u)$$

or

$$\left[\frac{dw}{d(r+u)} \right]^2 = \frac{1}{\left[\frac{2h\sigma_r}{p(r+u)} \right]^2 - 1} \quad (10)$$

Equation of strain. - Inasmuch as the element at radius r , defined by $\Delta\theta$ and Δr in the undeformed state, is moved to radius $r+u$, defined by $\Delta\theta$ and Δs , by the application of pressure p (fig. 1), by use of equation (8) the strains are

$$\epsilon_r = \log_e \frac{ds}{dr}$$

$$\epsilon_\theta = \log_e \frac{r+u}{r}$$

$$\epsilon_z = \log_e \frac{h}{h_1}$$

Then

$$\epsilon_r = \frac{d(r+u)}{dr} \left\{ 1 + \left[\frac{dw}{d(r+u)} \right]^2 \right\}^{1/2} \quad (11a)$$

$$\epsilon_\theta = \frac{r+u}{r} \quad (11b)$$

$$\epsilon_z = \frac{h}{h_1} \quad (11c)$$

Rotating Disk

Equation of equilibrium. - A disk of radius b and thickness h , rotating about its axis with angular speed ω , and an element taken at radius $r+u$, defined by $\Delta\theta$ and $\Delta(r+u)$, is shown in figure 3 with all the external forces acting on it. Summing up all forces acting on the element in the radial direction yields

$$\begin{aligned}
 & \sigma_r (r+u) h \Delta\theta - (\sigma_r + \Delta\sigma_r) \left[r+u + \Delta(r+u) \right] \Delta\theta (h+\Delta h) + \\
 & 2\sigma_\theta \left[\Delta(r+u) \right] \left(h + \frac{1}{2} \Delta h \right) \sin \frac{\Delta\theta}{2} - \\
 & \omega^2 \left[r+u + \frac{1}{2} \Delta(r+u) \right] \frac{\rho\pi \left[(r+\Delta r)^2 - r^2 \right] \Delta\theta}{2\pi} h_1 \\
 & = 0
 \end{aligned}$$

When $\Delta(r+u)$ approaches zero as a limit, the following equation of equilibrium is obtained:

$$r+u \frac{d(\sigma_r h)}{d(r+u)} = (\sigma_\theta - \sigma_r) h - \omega^2 r^2 h_1 \frac{r+u}{r} \frac{dr}{d(r+u)} \quad (12)$$

Equation of strains. - The strains are

$$\epsilon_r = \log_e \frac{d(r+u)}{dr}$$

$$\epsilon_\theta = \log_e \frac{r+u}{r}$$

$$\epsilon_z = \log_e \frac{h}{h_1}$$

therefore

$$e^{\epsilon_r} = \frac{d(r+u)}{dr} \quad (13a)$$

$$e^{\epsilon_\theta} = \frac{r+u}{r} \quad (13b)$$

$$e^{\epsilon_z} = \frac{h}{h_1} \quad (13c)$$

Infinite Plate with Circular Hole or Flat Ring Radially Stressed

An infinite plate uniformly stressed in its plane in all directions and having a circular hole is shown in figure 4. The whole system is equivalent to a very large circular plate of radius c with a small concentric circular hole radially subjected to the same uniform stress σ on the outer boundary. The solution obtained in such a plate within any radius b can also be considered as a solution of a flat ring with outer radius b and inner radius a , that is, uniformly loaded at the outer boundary with the radial stress σ_b obtained in the plate solution.

The equations for this case can be obtained in a manner similar to the two previous cases, or by simply setting dw/dr and w equal to zero in the case of the membrane, or setting ω equal to zero in the case of the rotating disk.

EQUATIONS OF EQUILIBRIUM AND COMPATIBILITY IN

TERMS OF PRINCIPAL STRESSES AND STRAINS

Circular Membrane under Pressure

By combining the equations previously derived the following set of independent equations, which define the problem, are obtained:

$$\epsilon_r = \frac{1}{3} \frac{\gamma}{\tau} \left(\sigma_r - \frac{1}{2} \sigma_\theta \right) \quad (6a)$$

$$\epsilon_\theta = \frac{1}{3} \frac{\gamma}{\tau} \left(\sigma_\theta - \frac{1}{2} \sigma_r \right) \quad (6b)$$

$$\epsilon_z = \frac{1}{3} \frac{\gamma}{\tau} \left[-\frac{1}{2} (\sigma_\theta + \sigma_r) \right] \quad (6c)$$

$$\gamma = 2\sqrt{\frac{2}{3}} \left(\epsilon_r^2 + \epsilon_\theta^2 + \epsilon_z^2 \right)^{1/2} \quad (5b)$$

$$\tau = \tau(\gamma) \quad (3)$$

$$e^{\epsilon_r} = \frac{d(r+u)}{dr} \left\{ 1 + \left[\frac{dw}{d(r+u)} \right]^2 \right\}^{1/2} \quad (11a)$$

$$e^{\epsilon_\theta} = \frac{r+u}{r} \quad (11b)$$

$$e^{\epsilon_z} = \frac{h}{h_1} \quad (11c)$$

$$(r+u) \frac{d(\sigma_r h)}{d(r+u)} = h(\sigma_\theta - \sigma_r) \quad (9)$$

$$\left[\frac{dw}{d(r+u)} \right]^2 = \frac{1}{\left[\frac{2h\sigma_r}{p(r+u)} \right]^2 - 1} \quad (10)$$

These equations are 10 independent relations of the 10 unknowns σ_r , σ_θ , ϵ_r , ϵ_θ , ϵ_z , γ , τ , h , u , and w .

If equation (11b) is differentiated with respect to r and combined with equation (11a),

$$r \frac{d\epsilon_\theta}{dr} = \frac{e^{(\epsilon_r - \epsilon_\theta)}}{\left\{ 1 + \left[\frac{dw}{d(r+u)} \right]^2 \right\}^{1/2}} - 1 \quad (14)$$

Substituting equation (10) in equation (14) to eliminate w yields following equation of compatibility:

$$r \frac{d\epsilon_\theta}{dr} = e^{(\epsilon_r - \epsilon_\theta)} \left\{ 1 - \left[\frac{p(r+u)}{2h\sigma_r} \right]^2 \right\}^{1/2} - 1 \quad (15)$$

Equations (9) and (15) can be simplified by using equations (11) to eliminate u and h , which results in

$$r \frac{d\sigma_r}{dr} + \sigma_r r \frac{d\epsilon_z}{dr} = (\sigma_\theta - \sigma_r) e^{(\epsilon_r - \epsilon_\theta)} \left\{ 1 - \left[\frac{r p e^{(\epsilon_\theta - \epsilon_z)}}{2 h_1 \sigma_r} \right]^2 \right\}^{1/2} \quad (16)$$

and

$$r \frac{d\epsilon_\theta}{dr} = e^{(\epsilon_r - \epsilon_\theta)} \left\{ 1 - \left[\frac{r p e^{(\epsilon_\theta - \epsilon_z)}}{2 h_1 \sigma_r} \right]^2 \right\}^{1/2} - 1 \quad (17)$$

The ten equations defining this problem are now reduced to seven independent equations, (6a), (6b), (6c), (5b), (3), (16), and (17), with the seven unknowns σ_r , σ_θ , ϵ_r , ϵ_θ , ϵ_z , τ , and γ .

The solution of the problem is simplified by further reducing equations (16) and (17) to the following forms:

$$\left. \begin{aligned} \frac{r}{k} \frac{d\sigma_r}{d\left(\frac{r}{k}\right)} + \sigma_r \frac{r}{k} \frac{d\epsilon_z}{d\left(\frac{r}{k}\right)} &= (\sigma_\theta - \sigma_r) e^{(\epsilon_r - \epsilon_\theta)} \left\{ 1 - \left[\frac{\frac{pk}{h_1} \frac{r}{k} e^{(\epsilon_\theta - \epsilon_z)}}{2\sigma_r} \right]^2 \right\}^{1/2} \\ \frac{r}{k} \frac{d\epsilon_\theta}{d\left(\frac{r}{k}\right)} &= e^{(\epsilon_r - \epsilon_\theta)} \left\{ 1 - \left[\frac{\frac{pk}{h_1} \frac{r}{k} e^{(\epsilon_\theta - \epsilon_z)}}{2\sigma_r} \right]^2 \right\}^{1/2} - 1 \end{aligned} \right\} \quad (18)$$

where k is any arbitrary unknown constant with the dimension of length. By using the two parameters r/k and pk/h_1 , it is then possible to solve the problem in a simple, direct way without use of the iteration method. This fact will be further discussed in the section METHODS OF NUMERICAL INTEGRATION.

Rotating Disk

The set of equations that define this problem are:

$$\epsilon_r = \frac{1}{3} \frac{\gamma}{\tau} (\sigma_r - \frac{1}{2} \sigma_\theta) \quad (6a)$$

$$\epsilon_\theta = \frac{1}{3} \frac{\gamma}{\tau} (\sigma_\theta - \frac{1}{2} \sigma_r) \quad (6b)$$

$$\epsilon_z = \frac{1}{3} \frac{\gamma}{\tau} \left[-\frac{1}{2} (\sigma_r + \sigma_\theta) \right] \quad (6c)$$

$$\gamma = 2 \sqrt{\frac{2}{3}} (\epsilon_r^2 + \epsilon_r \epsilon_\theta + \epsilon_\theta^2)^{1/2} \quad (5b)$$

$$\tau = \tau(\gamma) \quad (3)$$

$$e^{\epsilon_r} = \frac{d(r+u)}{dr} \quad (13a)$$

$$e^{\epsilon_\theta} = \frac{r+u}{r} \quad (13b)$$

$$e^{\epsilon_z} = \frac{h}{h_1} \quad (13c)$$

$$r+u \frac{d(\sigma_r h)}{d(r+u)} = h(\sigma_\theta - \sigma_r) - \rho \omega^2 r^2 h_1 \frac{r+u}{r} \frac{dr}{d(r+u)} \quad (12)$$

These equations are nine independent relations of the nine unknowns σ_r , σ_θ , ϵ_r , ϵ_θ , ϵ_z , γ , τ , h , and u . If equation (13b) is differentiated with respect to r and combined with equation (13a), the following compatibility equation is obtained:

$$r \frac{d\epsilon_\theta}{dr} = e^{(\epsilon_r - \epsilon_\theta)} - 1 \quad (19)$$

As in the case of the membrane, u and h can be eliminated from the equilibrium equation (12) by using equations (13), which yield

$$r \frac{d\sigma_r}{dr} + \sigma_r r \frac{d\epsilon_z}{dr} = (\sigma_\theta - \sigma_r) e^{(\epsilon_r - \epsilon_\theta)} - \rho \omega^2 r^2 e^{(-\epsilon_z)} \quad (20)$$

The nine equations defining this problem are now reduced to seven independent equations (6a), (6b), (6c), (5b), (3), (19), and (20), with seven unknowns σ_r , σ_θ , ϵ_r , ϵ_θ , ϵ_z , τ , and γ .

The solution of the problem is made simpler by further reducing equations (19) and (20) to the following forms:

$$\left. \begin{aligned} \frac{r}{k} \frac{d\sigma_r}{d\left(\frac{r}{k}\right)} + \sigma_r \frac{r}{k} \frac{d\epsilon_z}{d\left(\frac{r}{k}\right)} &= (\sigma_\theta - \sigma_r) e^{(\epsilon_r - \epsilon_\theta)} - \rho(\omega k)^2 \left(\frac{r}{k}\right)^2 e^{(-\epsilon_z)} \\ \frac{r}{k} \frac{d\epsilon_\theta}{d\left(\frac{r}{k}\right)} &= e^{(\epsilon_r - \epsilon_\theta)} - 1 \end{aligned} \right\} \quad (21)$$

By using the parameters r/k and ωk instead of r and ω , a simple direct solution is possible for any arbitrary value of ωk with k to be determined by the boundary condition.

Infinite Plate with Circular Hole or Flat Ring Radially Stressed

The equations of equilibrium and compatibility for this case are:

$$\left. \begin{aligned} \frac{r}{k} \frac{d\sigma_r}{d\left(\frac{r}{k}\right)} + \sigma_r \frac{r}{k} \frac{d\epsilon_z}{d\left(\frac{r}{k}\right)} &= (\sigma_\theta - \sigma_r) e^{(\epsilon_r - \epsilon_\theta)} \\ \frac{r}{k} \frac{d\epsilon_\theta}{d\left(\frac{r}{k}\right)} &= e^{(\epsilon_r - \epsilon_\theta)} - 1 \end{aligned} \right\} \quad (22)$$

When equations (22) are combined with equations (6a), (6b), (6c), (5b), and (3), there are seven equations with seven unknowns.

EQUATIONS OF EQUILIBRIUM AND COMPATIBILITY IN TERMS OF
OCTAHEDRAL SHEAR STRAIN AND PARAMETER INDICATING
RATIO OF PRINCIPAL STRESSES

In the preceding section, displacements are eliminated from the equations, which result in seven equations involving the seven unknown quantities σ_r , σ_θ , ϵ_r , ϵ_θ , ϵ_z , τ , and γ . The quantity ϵ_z can be expressed in terms of ϵ_r and ϵ_θ (from equation (1)). Two of the four unknowns σ_r , σ_θ , ϵ_r , and ϵ_θ may be eliminated by using equations (6a) and (6b) or (7). The quantity τ is a known function of γ that is experimentally determined. The problem is then reduced to one involving three unknowns. Obtaining the solution of the resulting equations is not, however, a simple matter.

It is proposed that this difficulty can be avoided by using the following transformation:

$$\sigma_\theta + \sigma_r = 3\sqrt{2}\tau \sin \alpha$$

$$\sigma_\theta - \sigma_r = \sqrt{6}\tau \cos \alpha$$

or

$$\left. \begin{aligned} \sigma_r &= \sqrt{\frac{3}{2}}\tau (\sqrt{3} \sin \alpha - \cos \alpha) \\ \sigma_\theta &= \sqrt{\frac{3}{2}}\tau (\sqrt{3} \sin \alpha + \cos \alpha) \end{aligned} \right\} \quad (23)$$

Then σ_r and σ_θ satisfy equation (5a). The octahedral shear stress τ , a function of γ , in the preceding equations varies with r/k and also with loading. Such a transformation has been used for the ideally plastic material ($\tau = \text{constant}$) by Nadai in the section "Yielding in Thin Plate with Circular Hole or Flat Rings Radially Stressed" (reference 1, p. 189) and for a rotating disk (reference 2). From equations (6a), (6b), and (23), the principal strains can be also expressed in terms of γ and α :

$$\left. \begin{aligned} \epsilon_r &= \frac{\gamma}{2\sqrt{2}} (\sin \alpha - \sqrt{3} \cos \alpha) \\ \epsilon_\theta &= \frac{\gamma}{2\sqrt{2}} (\sin \alpha + \sqrt{3} \cos \alpha) \end{aligned} \right\} \quad (24)$$

The equations of equilibrium and compatibility for the three problems considered here are then obtained in terms of γ and α in the following form:

$$\left. \begin{aligned} A \frac{r}{k} \frac{d\alpha}{d\left(\frac{r}{k}\right)} + B \frac{r}{k} \frac{d\gamma}{d\left(\frac{r}{k}\right)} &= C \\ D \frac{r}{k} \frac{d\alpha}{d\left(\frac{r}{k}\right)} + E \frac{r}{k} \frac{d\gamma}{d\left(\frac{r}{k}\right)} &= F \end{aligned} \right\} \quad (25)$$

where the coefficients A , B , C , D , E , and F are functions of α , γ , and r/k . For the circular membrane under pressure, from equation (18),

$$\left. \begin{aligned} A &= (\sqrt{3} \cos \alpha + \sin \alpha) - (\sqrt{3} \sin \alpha - \cos \alpha) \frac{\gamma \cos \alpha}{\sqrt{2}} \\ B &= (\sqrt{3} \sin \alpha - \cos \alpha) \left(\frac{\gamma}{\tau} \frac{d\tau}{d\gamma} - \frac{\gamma \sin \alpha}{\sqrt{2}} \right) \frac{1}{\gamma} \\ C &= 2(\cos \alpha) e^{(-\sqrt{\frac{3}{2}} \gamma \cos \alpha)} \left[1 - \frac{e^{\sqrt{\frac{3}{2}} (\sqrt{3} \sin \alpha + \cos \alpha) \gamma}}{6\tau^2 (\sqrt{3} \sin \alpha - \cos \alpha)^2} \left(\frac{r}{k} \right)^2 \left(\frac{pk}{h_1} \right)^2 \right]^{1/2} \\ D &= (\sqrt{3} \sin \alpha - \cos \alpha) \gamma \\ E &= -(\sqrt{3} \cos \alpha + \sin \alpha) \\ F &= 2\sqrt{2} \left\{ 1 - e^{(-\sqrt{\frac{3}{2}} \gamma \cos \alpha)} \left[1 - \frac{e^{\sqrt{\frac{3}{2}} (\sqrt{3} \sin \alpha + \cos \alpha) \gamma}}{6\tau^2 (\sqrt{3} \sin \alpha - \cos \alpha)^2} \left(\frac{r}{k} \right)^2 \left(\frac{pk}{h_1} \right)^2 \right]^{1/2} \right\} \end{aligned} \right\} \quad (26)$$

For the rotating disk, from equation (21),

$$\left. \begin{aligned}
 A &= (\sqrt{3} \cos \alpha + \sin \alpha) - (\sqrt{3} \sin \alpha - \cos \alpha) \frac{\gamma \cos \alpha}{\sqrt{2}} \\
 B &= (\sqrt{3} \sin \alpha - \cos \alpha) \left(\frac{\gamma}{\tau} \frac{d\tau}{d\gamma} - \frac{\gamma \sin \alpha}{\sqrt{2}} \right) \frac{1}{\gamma} \\
 C &= 2(\cos \alpha) e^{\left(-\sqrt{\frac{3}{2}} \gamma \cos \alpha \right)} - \sqrt{\frac{2}{3}} \rho (\omega k)^2 \frac{1}{\tau} \left(\frac{r}{k} \right)^2 e^{\frac{\gamma}{\sqrt{2}} \sin \alpha} \\
 D &= (\sqrt{3} \sin \alpha - \cos \alpha) \gamma \\
 E &= -(\sqrt{3} \cos \alpha + \sin \alpha) \\
 F &= 2\sqrt{2} \left[1 - e^{\left(-\sqrt{\frac{3}{2}} \gamma \cos \alpha \right)} \right]
 \end{aligned} \right\} \quad (27)$$

For the infinite plate with a circular hole, from equation (22),

$$\left. \begin{aligned}
 A &= (\sqrt{3} \cos \alpha + \sin \alpha) - (\sqrt{3} \sin \alpha - \cos \alpha) \frac{\gamma \cos \alpha}{\sqrt{2}} \\
 B &= (\sqrt{3} \sin \alpha - \cos \alpha) \left(\frac{\gamma}{\tau} \frac{d\tau}{d\gamma} - \frac{\gamma \sin \alpha}{\sqrt{2}} \right) \frac{1}{\gamma} \\
 C &= 2(\cos \alpha) e^{\left(-\sqrt{\frac{3}{2}} \gamma \cos \alpha \right)} \\
 D &= (\sqrt{3} \sin \alpha - \cos \alpha) \gamma \\
 E &= -(\sqrt{3} \cos \alpha + \sin \alpha) \\
 F &= 2\sqrt{2} \left[1 - e^{\left(-\sqrt{\frac{3}{2}} \gamma \cos \alpha \right)} \right]
 \end{aligned} \right\} \quad (28)$$

With these transformations, the solution of the problems is reduced to simply a numerical integration of the two simultaneous differential equations (equations (25)) involving the two unknowns γ and α .

Furthermore, the parameter γ , being the octahedral shear strain, directly indicates the stage of plastic deformation at any point under any load. (In plastic problems, according to the deformation theory, the individual stress and strain distribution cannot give as clear a picture of the stage of plastic deformation as can the octahedral shear strain.) Also, the parameter α indicates the ratio of the principal stresses or strains. At any point, if α remains constant during loading, the ratio of principal stresses at that point remains fixed. The value of α obtained at each point in the calculation during loading directly indicates whether or not the deformation theory is applicable to the problem.

The value of α is known at the boundaries or the center. From equations (23) and (24), in the case of a circular membrane under pressure,

when $r/b = 0$,

$$\sigma_r = \sigma_\theta$$

$$\alpha = \frac{\pi}{2} = 1.5708$$

when $r/b = 1$,

$$\epsilon_\theta = 0$$

$$\alpha = \frac{2}{3} \pi = 2.0944$$

In the case of a rotating disk without a hole,

when $r/b = 0$,

$$\sigma_r = \sigma_\theta$$

$$\alpha = \frac{\pi}{2} = 1.5708$$

when $r/b = 1$,

$$\sigma_r = 0$$

$$\alpha = \frac{\pi}{6} = 0.5236$$

In the case of a rotating disk with a hole,
when $r/a = 1$ and $r/b = 1$,

$$\sigma_r = 0$$

$$\alpha = \frac{\pi}{6} = 0.5236$$

For the infinite plate with a circular hole,
when $r/a = 1$,

$$\sigma_r = 0$$

$$\alpha = \frac{\pi}{6} = 0.5236$$

when r/a approaches c/a or a value large compared with 1,

$$\sigma_r = \sigma_\theta$$

$$\alpha = \frac{\pi}{2} = 1.5708$$

EQUATIONS OF EQUILIBRIUM AND COMPATIBILITY FOR INFINITESIMAL STRAIN

IN TERMS OF α AND γ

The final forms of the equilibrium and compatibility equations for the case of small strains are given in this section. The concept of infinitesimal strain is defined as follows: The change of dimensions are small compared with the original dimensions, but are large enough so that the elastic strain can be neglected. The equations presented can be obtained either by direct derivation as was previously done or by reducing from the equations for finite strains through expanding the $e^{\pm(\alpha, \gamma)}$ terms in series and neglecting the small terms. For infinitesimal strain, the coefficients (functions of α and γ) A, B, C, D, E, and F in the preceding equations are denoted with a superscript prime in similar forms, but the coefficient (functions of α and γ) are simpler than those for large strain.

$$A' \frac{r}{k} \frac{d\alpha}{d\left(\frac{r}{k}\right)} + B' \frac{r}{k} \frac{d\gamma}{d\left(\frac{r}{k}\right)} = C'$$

(29)

$$D' \frac{r}{k} \frac{d\alpha}{d\left(\frac{r}{k}\right)} + E' \frac{r}{k} \frac{d\gamma}{d\left(\frac{r}{k}\right)} = F'$$

For the circular membrane under pressure,

$$\left. \begin{aligned} A' &= \sqrt{3} \cos \alpha + \sin \alpha \\ B' &= (\sqrt{3} \sin \alpha - \cos \alpha) \frac{1}{\tau} \frac{d\tau}{d\gamma} \\ C' &= 2 \cos \alpha \\ D' &= (\sqrt{3} \sin \alpha - \cos \alpha) \gamma \\ E' &= -(\sqrt{3} \cos \alpha + \sin \alpha) \\ F' &= 2\sqrt{3} \gamma \cos \alpha + \frac{\sqrt{2}}{6} \left[\frac{\frac{pk}{h_1} \frac{r}{k}}{\tau(\sqrt{3} \sin \alpha - \cos \alpha)} \right]^2 \end{aligned} \right\} \quad (30)$$

For the rotating disk,

$$\left. \begin{aligned} A' &= \sqrt{3} \cos \alpha + \sin \alpha \\ B' &= (\sqrt{3} \sin \alpha - \cos \alpha) \frac{1}{\tau} \frac{d\tau}{d\gamma} \\ C' &= 2 \cos \alpha - \sqrt{\frac{2}{3}} \rho (\omega k)^2 \left(\frac{r}{k}\right)^2 \frac{1}{\tau} \\ D' &= (\sqrt{3} \sin \alpha - \cos \alpha) \gamma \\ E' &= -(\sqrt{3} \cos \alpha + \sin \alpha) \\ F' &= 2\sqrt{3} (\cos \alpha) \gamma \end{aligned} \right\} \quad (31)$$

For the infinite plate with a circular hole,

$$\left. \begin{aligned} A' &= \sqrt{3} \cos \alpha + \sin \alpha \\ B' &= (\sqrt{3} \sin \alpha - \cos \alpha) \frac{1}{r} \frac{dr}{d\gamma} \\ C' &= 2 \cos \alpha \\ D' &= (\sqrt{3} \sin \alpha - \cos \alpha) \\ E' &= -(\sqrt{3} \cos \alpha + \sin \alpha) \\ F' &= 2\sqrt{3} (\cos \alpha) \gamma \end{aligned} \right\} \quad (32)$$

METHODS OF NUMERICAL INTEGRATION

Two methods are developed to solve the differential equations (25). In the first method, the differential equations are numerically integrated along r/k , which is considered the independent variable. In the second method, α is considered the independent variable. Because many terms in the equations are trigonometric functions of α , the use of α as the independent variable considerably reduces the work of computation.

Numerical integration with r/k as independent variable. -
Equations (25) can be written in the following forms:

$$\left. \begin{aligned} \frac{r}{k} \frac{d\alpha}{d\left(\frac{r}{k}\right)} &= \frac{CE-FB}{AE-DB} \\ \frac{r}{k} \frac{d\gamma}{d\left(\frac{r}{k}\right)} &= \frac{FA-CD}{EA-BD} \end{aligned} \right\} \quad (33)$$

For the case of small strain, the terms A' , B' , C' , D' , E' , and F' are used in equation (33) instead of A , B , C , D , E , and F , respectively. If at any point α and γ are known, $\frac{d\alpha}{d(r/k)}$ and $\frac{d\gamma}{d(r/k)}$ can be calculated by equations (33). At the boundaries or the center, α is known, but γ is to be determined by the load. Only

one value (unknown) of γ corresponding to a particular load exists on each boundary. It is therefore difficult to start the numerical integrations on the boundary with the correct value of γ corresponding to a given load. Also, in plastic problems covering the strain-hardening range, the method of superposition is invalid. Usually, a method of iteration is used to solve the problem (for example, reference 3). In the method presented herein, an arbitrary but unknown constant k has been introduced in equations (18), (21), and (22). For the cases considered, the terms in the equations that involve load are always multiplied by r , so that $\left(\frac{pr}{h_1}\right)^2$ can be written as $\left(\frac{pk}{h_1}\right)^2 \left(\frac{r}{k}\right)^2$ in equations (18) and (26) and $(\omega r)^2$ as $(\omega k)^2 \left(\frac{r}{k}\right)^2$ in equations (21) and (27).

The numerical integration can then be started at the inner boundary (or at the center if there is no circular hole at the center) by using the known values of α_0 , a desired value of γ_0 , and arbitrary value of $\left(\frac{pk}{h_1}\right)^2$ for the membrane or of $(\omega k)^2$ for the rotating disk. The numerical integrations can then be carried out, obtaining values of α and γ at different values of r/k , until α progressively reaches the value that satisfies the other boundary condition. Because the value of r is known at the boundaries, the value of k can be determined for the selected value of γ_0 . The number of points and the formulas used in the calculation depend on the accuracy required (references 19 and 20). It has been found that if the formula for evaluating definite integrals is applied after using the forward integration formula (references 19 and 20), high accuracy can easily be obtained.

The procedure used herein to obtain solutions is the same for each problem. Calculations are started from the inner boundary (or from the center if there is no circular hole at the center) with the known value of α_0 , the desired value of γ_0 , and the arbitrary loading term. The parameter α_0 is equal to $\pi/2$ at $r/b = 0$ for the membrane and for the solid rotating disk and is equal to $\pi/6$ at $r/a = 1$ for the infinite plate with a circular hole and for the rotating disk with a hole. The arbitrary loading terms are $\left(\frac{pk}{h_1}\right)^2$ and $(\omega k)^2$ for the membrane and the rotating disk, respectively. Then $\left[\frac{d\alpha}{d(r/k)}\right]_0$ and

$\left[\frac{d\gamma}{d(r/k)}\right]_0$, corresponding to α_0 and γ_0 at the inner boundary or the

center, are obtained from equation (33). The following formulas for forward integration are used to determine the first approximate values of α and γ at the next point (α_1^* and γ_1^*):

$$\left. \begin{aligned} \alpha_1^* &= \alpha_0 + \left[\left(\frac{r}{k} \right)_1 - \left(\frac{r}{k} \right)_0 \right] \left[\frac{d\alpha}{d\left(\frac{r}{k} \right)} \right]_0 \\ \gamma_1^* &= \gamma_0 + \left[\left(\frac{r}{k} \right)_1 - \left(\frac{r}{k} \right)_0 \right] \left[\frac{d\gamma}{d\left(\frac{r}{k} \right)} \right]_0 \end{aligned} \right\} \quad (34a)$$

By substituting α_1^* and γ_1^* into equation (33), approximate values of $\left[\frac{d\alpha}{d\left(\frac{r}{k} \right)} \right]_1$ and $\left[\frac{d\gamma}{d\left(\frac{r}{k} \right)} \right]_1$ are obtained and the second approximate values of α_1 and γ_1 (α_1^{**} and γ_1^{**}) can be computed from the following formulas:

$$\left. \begin{aligned} \alpha_1^{**} &= \alpha_0 + \frac{1}{2} \left[\left(\frac{r}{k} \right)_1 - \left(\frac{r}{k} \right)_0 \right] \left\{ \left[\frac{d\alpha}{d\left(\frac{r}{k} \right)} \right]_0 + \left[\frac{d\alpha}{d\left(\frac{r}{k} \right)} \right]_1^* \right\} \\ \gamma_1^{**} &= \gamma_0 + \frac{1}{2} \left[\left(\frac{r}{k} \right)_1 - \left(\frac{r}{k} \right)_0 \right] \left\{ \left[\frac{d\gamma}{d\left(\frac{r}{k} \right)} \right]_0 + \left[\frac{d\gamma}{d\left(\frac{r}{k} \right)} \right]_1^* \right\} \end{aligned} \right\} \quad (34b)$$

The values of α_1^{**} and γ_1^{**} are substituted into equation (33) again in order to calculate the values of $\left[\frac{d\alpha}{d\left(\frac{r}{k} \right)} \right]_1$ and $\left[\frac{d\gamma}{d\left(\frac{r}{k} \right)} \right]_1$. By use of

the following formulas for evaluating definite integrals, the values of α_1 and γ_1 are calculated:

$$\left. \begin{aligned} \alpha_1 &= \alpha_0 + \frac{1}{2} \left[\left(\frac{r}{k} \right)_1 - \left(\frac{r}{k} \right)_0 \right] \left\{ \left[\frac{d\alpha}{d\left(\frac{r}{k} \right)} \right]_0 + \left[\frac{d\alpha}{d\left(\frac{r}{k} \right)} \right]_1 \right\} \\ \gamma_1 &= \gamma_0 + \frac{1}{2} \left[\left(\frac{r}{k} \right)_1 - \left(\frac{r}{k} \right)_0 \right] \left\{ \left[\frac{d\gamma}{d\left(\frac{r}{k} \right)} \right]_0 + \left[\frac{d\gamma}{d\left(\frac{r}{k} \right)} \right]_1 \right\} \end{aligned} \right\} \quad (34c)$$

This procedure is applied to the next point, and so forth, until the value of α reaches the required value of α_b at the outside boundary ($\alpha_b = 2/3 \pi$ at $r/b = 1$ for the membrane, $\alpha_b = \pi/6$ at $r/b = 1$ for the rotating disk, and $\alpha_b = \pi/2$ at $r/a = c/a$ for the thin plate with a circular hole). Inasmuch as

$$\left(\frac{r}{k}\right)_{\alpha=\alpha_b} = \frac{b}{k}$$

the loading terms are determined as follows:

For the membrane,

$$\left(\frac{pb}{h_1}\right)^2 = \left(\frac{pk}{h_1}\right)^2 \left(\frac{b}{k}\right)^2 \quad (33a)$$

For the rotating disk,

$$(\omega b)^2 = (\omega k)^2 \left(\frac{b}{k}\right)^2 \quad (33b)$$

For the infinite plate with a circular hole,

$$t_c = \sigma h_c \left(\frac{r+u}{r}\right)_c = \sigma h_1 e^{-\epsilon_r} = \sigma h_1 e^{-\frac{\gamma_c}{2\sqrt{2}}} \quad (33c)$$

or for the flat ring radially stressed at the outside diameter b ,

$$t_b = (\sigma_r)_b h_b \left(\frac{r+u}{r}\right)_b = (\sigma_r)_b h_1 e^{-\frac{\gamma_b}{2\sqrt{2}} (\sin \alpha_b - \sqrt{3} \cos \alpha_b)} \quad (33d)$$

where t_c and t_b are the tension per unit original circumferential length at $r = c$ and $r = b$, respectively.

Numerical integration with α as independent variable. -
Equations (33) can be written in the following forms:

$$\left. \begin{aligned} \frac{d\gamma}{d\alpha} &= \frac{FA-CD}{CE-FB} \\ \frac{d\left(\frac{r}{k}\right)}{d\alpha} &= \frac{AE-DB}{CE-BF} \frac{r}{k} \end{aligned} \right\} \quad (35)$$

By using equations (26) to (28) and expanding $e^{f(\alpha, \gamma)}$ into a series, the following equations are obtained:

For the circular membrane, from equations (26),

$$\left. \begin{aligned} CE-BF &= 2GJ - \left[2\sqrt{3}HJ \, g\left(\alpha, \gamma, \frac{\gamma}{\tau} \frac{d\tau}{d\gamma}\right) f_1(\alpha, \gamma) + 2\sqrt{3} \right] j\left(\alpha, \gamma, \frac{r}{k}, \frac{pk}{h_1}\right) \\ AF-CD &= 2\sqrt{2}L - 2HJ \, \gamma - 2\sqrt{2}L \, f_2(\alpha, \gamma) \, j\left(\alpha, \gamma, \frac{r}{k}, \frac{pk}{h_1}\right) \\ AE-BD &= -L^2 - J^2 \, g\left(\alpha, \gamma, \frac{\gamma}{\tau} \frac{d\tau}{d\gamma}\right) \end{aligned} \right\} \quad (36)$$

For the rotating disk, from equations (27),

$$\left. \begin{aligned} CE-BF &= -2HL - 2\sqrt{3}HJ \, g\left(\alpha, \gamma, \frac{\gamma}{\tau} \frac{d\tau}{d\gamma}\right) f_1(\alpha, \gamma) + L \frac{K_2}{\tau} \left(\frac{r}{k}\right)^2 f_3(\alpha, \gamma) \\ AF-CD &= \left\{ 8H^2 - 2\sqrt{3}HL \left[1 - f_1(\alpha, \gamma) \right] + J \frac{K_2}{\tau} \left(\frac{r}{k}\right)^2 f_3(\alpha, \gamma) \right\} \gamma \\ AE-BD &= -L^2 - J^2 \, g\left(\alpha, \gamma, \frac{\gamma}{\tau} \frac{d\tau}{d\gamma}\right) \end{aligned} \right\} \quad (37)$$

For the infinite plate with a circular hole, from equations (28),

$$\left. \begin{aligned} CE-BF &= -2HL - 2\sqrt{3}HJ \, g\left(\alpha, \gamma, \frac{\gamma}{\tau} \frac{d\tau}{d\gamma}\right) f_1(\alpha, \gamma) \\ AF-CD &= \left\{ 8H^2 - 2\sqrt{3}HL \left[1 - f_1(\alpha, \gamma) \right] \right\} \gamma \\ AF-BD &= -L^2 - J^2 \, g\left(\alpha, \gamma, \frac{\gamma}{\tau} \frac{d\tau}{d\gamma}\right) \end{aligned} \right\} \quad (38)$$

where

$$G = \sin \alpha$$

$$H = \cos \alpha$$

$$J = \sqrt{3} \sin \alpha - \cos \alpha$$

$$L = \sqrt{3} \cos \alpha + \sin \alpha$$

$$K_1 = \left(\frac{pk}{h_1} \right)^2$$

$$K_2 = \sqrt{\frac{2}{3}} \, \rho(\omega k)^2$$

and

$$f_1(\alpha, \gamma) = \frac{1}{\sqrt{\frac{3}{2}}(\cos \alpha)\gamma} \left[1 - e^{-\sqrt{\frac{3}{2}}(\cos \alpha)\gamma} \right]$$

$$= 1 - \frac{1}{2} \sqrt{\frac{3}{2}}(\cos \alpha)\gamma + \frac{1}{4}(\cos^2 \alpha)\gamma^2 - \dots$$

$$f_2(\alpha, \gamma) = e^{-\sqrt{\frac{3}{2}}(\cos \alpha)\gamma}$$

$$= 1 - \sqrt{\frac{3}{2}}(\cos \alpha)\gamma + \frac{1}{2} \times \frac{3}{2}(\cos^2 \alpha)\gamma^2 - \frac{1}{4} \sqrt{\frac{3}{2}}(\cos^3 \alpha)\gamma^3 + \dots$$

$$= 1 - \sqrt{\frac{3}{2}}(\cos \alpha)\gamma f_1(\alpha, \gamma)$$

$$f_3(\alpha, \gamma) = e^{\frac{\gamma}{\sqrt{2}} \sin \alpha}$$

$$= 1 + \left(\frac{1}{\sqrt{2}} \sin \alpha \right) \gamma + \frac{1}{2} \left(\frac{1}{\sqrt{2}} \sin \alpha \right)^2 \gamma^2 + \frac{1}{6} \left(\frac{1}{\sqrt{2}} \sin \alpha \right)^3 \gamma^3 + \dots$$

$$g\left(\alpha, \gamma, \frac{\gamma}{\tau} \frac{d\tau}{d\gamma}\right) = \frac{\gamma}{\tau} \frac{d\tau}{d\gamma} - \sqrt{\frac{3}{2}} \frac{\gamma}{\sqrt{3} \sin \alpha - \cos \alpha}$$

$$= \frac{\gamma}{\tau} \frac{d\tau}{d\gamma} - \sqrt{\frac{3}{2}} \frac{\gamma}{J}$$

$$j\left(\alpha, \gamma, \frac{r}{k}, \frac{pk}{h_1}\right) = \left[1 - \frac{e^{\sqrt{\frac{3}{2}} \gamma (\sqrt{3} \sin \alpha + \cos \alpha)}}{6\tau^2 (\sqrt{3} \sin \alpha - \cos \alpha)^2} \left(\frac{r}{k}\right)^2 \left(\frac{pk}{h_1}\right)^2 \right]^{1/2}$$

$$= \left[1 - \frac{K_1}{6J^2} \left(\frac{1}{\tau} \frac{r}{k}\right)^2 \frac{f_3(\alpha, \gamma)}{f_2(\alpha, \gamma)} \right]^{1/2}$$

The symbols G , H , J , and L are trigonometric functions of α only; K_1 and K_2 are constants during calculation. The symbols f_1 , f_2 , f_3 , and g are functions of α and γ ; j is a function of α , γ , and $\frac{r}{k}$.

This method is used herein in the solution of an infinite plate with a circular hole. The procedure of numerical integration is similar to that used in the first method. The first four terms of the series of $e^{f(\alpha, \gamma)}$ are used; the accuracy of the result is the same as that in the first method, with a reduction of one half in computation.

Both methods presented herein are used to obtain the solutions for the given values of γ_0 . The purpose of the present paper is to obtain solutions for the entire strain-hardening range and the methods developed are very convenient for this purpose. If, however, a solution for only a particular value of loading is required, it can be obtained by interpolating between values obtained from two or three solutions corresponding to loading near the specified value.

NUMERICAL EXAMPLES

Membrane. - In order to compare the results obtained by the method developed herein to those obtained by Gleyzal (reference 3), one numerical solution for infinitesimal strain is calculated by using the $\tau(\gamma)$ curve of the tensile test in figure 1 of reference 3. Inasmuch as reference 3 states that: "For simplicity, strain will be taken to mean conventional strain $(ds-ds_0)/ds_0$ where ds and ds_0 are final and initial arc length, respectively.", equations (29) and (30) for infinitesimal strain are used. The calculation is started at $r/k = 0.005$. Values of $\alpha_0 = 1.5708$, $\gamma_0 = 0.0299$, and $pk/h_1 = 55,920$ are used.

Rotating disk. - Numerical solutions for finite strain (equations (25) and (27)) are calculated. The $\tau(\gamma)$ curves of two materials, Inconel X and 16-25-6, are plotted in figure 5(a). These data were supplied by W. F. Brown, Jr., H. Schwartzbart, and M. H. Jones. The same $\tau(\gamma)$ curves are plotted on logarithmic coordinates in figure 5(b). These materials, Inconel X and 16-25-6, of which τ is not a power function of γ , were chosen so that more general information can be obtained. It should be mentioned that the given octahedral shear stress-strain curves (fig. 5) of these two materials have not been corrected for the triaxiality and nonuniform stress distribution introduced by necking, and consequently do not represent the exact stress-strain relation after necking of these two materials. The solutions obtained from the $\tau(\gamma)$ curves of the tensile test after necking can, however, represent the solutions corresponding to materials having the exact $\tau(\gamma)$ curves shown in figure 5 and for simplicity the materials are herein still referred to as Inconel X and 16-25-6.

In each case, the calculation is started at $r/k = 0.005$, as in the case of a membrane.

Three solutions are also obtained for a rotating disk with a central hole, using Inconel X. Calculations are started at $r/a = 1$.

All numerical examples are given in the following table:

Solid rotating disk		
Material	γ_0	$\sqrt{\frac{2}{3}} \rho(\omega b)^2$
Inconel X	0.04	1×10^5
	.1152	1×10^5
	.30	1×10^5
16-25-6	0.04	1×10^5
	.1152	1×10^5
	.30	2.5×10^5

Rotating disk with central hole		
Material	γ_0	$\sqrt{\frac{2}{3}} \rho(\omega a)^2$
Inconel X	0.30	1×10^4
	.30	2×10^3
	.30	4×10^2

Infinite plate with circular hole. - The calculations for this problem are carried out for the case in which $\sigma_r = 0$ at $r/a = 1$. The value of α_0 at $r/a = 1$ is then 0.5236. (For other cases where σ_r is different from 0 at $r/a = 1$, the corresponding value of α_0 should be used.) The same materials as in the previous problem are considered. The numerical examples are:

Material	γ_0
Inconel X	0.04
	.1152
	.1871
	.30
16-25-6	0.04
	.1871
	.30

RESULTS AND DISCUSSION

The radial and circumferential stresses σ_r and σ_θ , respectively, obtained for the case of a circular membrane are plotted against r/b in figure 6. Two curves, taken from reference 3, corresponding to calculations for about the same pressure used in the present calculation, are included in the figure for comparison. In the present calculation, the $\gamma(\gamma)$ curve given in figure 1 of reference 3 and the same infinitesimal-strain definition based on the original dimension is used. In order to be consistent, the initial thickness h_1 is also used in the calculation rather than the instantaneous thickness h , which is used in reference 3.

The variations of α with the radius for the rotating disk and for the infinite plate with a circular hole for different loads and materials are plotted in figures 7(a) and 7(b), respectively. The variations of α with γ_0 (or loading) at various radii for the rotating disk and the infinite plate with a circular hole are plotted in figures 8(a) and 8(b), respectively. Similar curves for the ratio of the principal stresses σ_r/σ_θ are shown in figures 9(a), 9(b), and 10. When figure 7 is compared with figures 9(a) and 9(b), it is seen that the variations of α with radius are very similar to the variations of σ_r/σ_θ with radius, although the relation between α and σ_r/σ_θ is not linear.

Examples for a membrane with a large strain are not calculated herein, because the result of reference 3 is sufficient to give an approximate variation of the ratios of principal stresses along the radius during loading, although the infinitesimal-strain concept is used. The variations of the ratio of principal stresses with radius for different loads, based on the values of σ_r and σ_θ given in figures 8 and 9 of reference 3, are calculated and plotted on figure 9(c).

The values of σ_r are plotted against σ_θ at different radii under different loads for the rotating disk and the infinite plate with a circular hole in figure 11. The heavy solid and dashed curves represent the values of σ_r and σ_θ at different radii for any given load and are called loading curves. The loading curve moves away from the origin with increasing load. The light solid and dotted lines connecting the different loading curves at a given radius and extending to the origin represent the values of σ_r and σ_θ at different loads for any given radius and are called loading paths. Also shown in the figures are the yielding surfaces, which are ellipses under the deformation theory.

A clear picture of the variation of the ratios of principal stresses in this group of problems with different loads and with different materials is given in figures 7 to 11. It is evident that the ratios of principal stresses remain essentially constant during loading. For this group of problems, the deformation theory is therefore applicable and ϵ_j , defined by equation (8), represents the true strain and is determined by the final and initial states.

The variations of γ and γ/γ_0 with radius are plotted in figures 12 and 13, respectively, for the rotating disk and the infinite plate with circular hole. It is interesting to note that the curves in figure 13 for different loads for the same material are quite close. The curves for different materials on figures 7 and 9 are also close, but are not so close in figure 13.

The distributions of principal stresses and principal strains along the radius for the rotating disk and for the infinite plate with a circular hole are plotted in figures 14 and 15, respectively. For comparison, the variations of $\sigma_\theta/(\sigma_\theta)_0$, $\epsilon_\theta/(\epsilon_\theta)_0$, and γ/γ_0 with radius for both the elastic and the plastic range are plotted in figures 16 and 17. (The equations for the elastic range are given in the appendix.) If only the stress distributions for the elastic and plastic cases are compared, it is seen that the stresses are more uniform in the plastic state; but if the distributions of the principal strains and the octahedral shear strain for the elastic and the plastic cases are compared, it is evident that a less-uniform strain distribution is obtained in the plastic state. It is of special interest in the case of the finite plate with a hole to note that with plastic formation, the stress (tangential stress) concentration factor around the hole is reduced, but instead there is a high concentration in principal strain and in octahedral shear strain. A similar conclusion regarding concentration factor around a circular hole in a tension panel is obtained in references 21 and 22.

The quantities $\sigma_\theta/(\sigma_\theta)_0$, $\sigma_r/(\sigma_r)_0$, $\epsilon_r/(\epsilon_r)_0$, and $\epsilon_\theta/(\epsilon_\theta)_0$ along the radius for a rotating disk and $\sigma_\theta/(\sigma_\theta)_0$ and $\epsilon_\theta/(\epsilon_\theta)_0$ for an infinite plate with a circular hole are plotted in figures 18 and 19, respectively. The curves representing $\sigma_r/(\sigma_r)_0$, $\epsilon_r/(\epsilon_r)_0$, and $\epsilon_\theta/(\epsilon_\theta)_0$ for different materials and different values of γ_0 are close together; but the curves of $\sigma_\theta/(\sigma_\theta)_0$ are quite different for different materials, as well as for different values of γ_0 .

The relation between load and maximum octahedral shear strain γ_o of the rotating disk and the infinite plate with a hole are plotted in figure 20. The terms $\rho(\omega b)^2$ and t_b/h_1 are designated the load for the rotating disk and the infinite plate with a hole, respectively. It is shown in these figures that the load increases considerably for Inconel X when the value of γ_o increases from 0.04 to 0.30, whereas the load for 16-25-6 increases only slightly.

In figures 7, 13, and 16 to 19, it is shown that in the case of the plate with a hole, the variations of α , γ/γ_o , $\epsilon_r/(\epsilon_r)_o$, and $\epsilon_\theta/(\epsilon_\theta)_o$ with radius are essentially independent of the value of γ_o of the plate and the $\tau(\gamma)$ curve of the material, at least within the range of τ , γ variation enclosed by those values of the two materials used. From these results, it can be seen that the deformation that can be accepted by the plate before failure depends mainly on the maximum octahedral shear strain (or ductility) of the material, which would not be true if the strain distributions were a function of the τ - γ curve. In the case of the rotating disk, however, a slight effect of γ_o and the $\tau(\gamma)$ curve is apparent on the strains; this effect seems to be caused by the body-force term of the disk.

The stress distribution that will determine the load the member can sustain is now considered. From figures 16 to 19, it can be seen that the variations of $\sigma_\theta/(\sigma_\theta)_o$ with radius depend upon the $\tau(\gamma)$ curve of the material and on the value of γ_o of the member. From figure 20, it is also seen that the load depends on the $\tau(\gamma)$ curve. It therefore follows that the added load that the member can sustain between the onset of yielding and failure depends on the $\tau(\gamma)$ curve of the material. The octahedral shear (or effective) stress and strain curve of the material should therefore be used as a criterion in selecting a material for a certain member under a certain loading condition, because consideration of the maximum octahedral shear strain of the material alone (or ductility alone) is insufficient.

The variations of α , γ , σ_r , σ_θ , ϵ_r , ϵ_θ , and γ/γ_b with radius of three rotating disks with a hole are shown in figure 21. These three disks have the values of ratios of outer and inner radius b/a equal to 5.32, 12.45, and 28.12, respectively. The tangential stress σ_θ , the tangential strain ϵ_θ , and the octahedral shear strain γ are much less uniform than in the case of a solid rotating disk. The ratio of maximum and minimum octahedral shear strain γ_o/γ_b is equal to 7.41 for a disk with $b/a = 5.32$, equal to 11.75 for a disk with $b/a = 12.45$, and equal to 14.1 for a disk with $b/a = 28.12$; for a solid disk of the same material, the ratio γ_o/γ_b is about 5.3.

The values of the load, defined by $\rho(\omega b)^2$, for rotating disks having different ratios of inner to outer radius a/b are represented by the solid curve in figure 22. These disks were made of Inconel X and reach the same maximum octahedral shear strain $\gamma_0 = 0.3$ at the inner radius of the disk. The dashed curve in the same figure is obtained by extending this solid curve toward $a/b = 1$, where the value of $\rho(\omega b)^2$ can be determined by considering a rotating ring with $a/b \rightarrow 1$. The figure indicates approximately how the load $\rho(\omega b)^2$ varies with different disks having different ratios of inner and outer radius and reaching the same maximum octahedral shear strain at the inner radius of the disk. The value of $\rho(\omega b)^2$ for a solid rotating disk made of Inconel X with $\gamma_0 = 0.3$ at the center of the disk is also indicated in the same figure.

The preceding results and discussion were obtained for the plane-stress problems with axial symmetry in the strain-hardening range in which the elastic strains are negligible compared with the plastic strains. Whether these results and discussions are true for general two-dimensional or three-dimensional problems, or for the problems involving the region in which elastic strain is not small compared with plastic strain, or for partly plastic problems, can be determined only by a detailed analysis of each case.

CONCLUSIONS

The results obtained in the cases of a membrane, a rotating disk without and with a hole, and an infinite plate with a hole in the strain-hardening range of two materials, Inconel X and 16-25-6, whose stress-strain relations do not follow the power law, show that:

- (1) The method developed not only accurately solved the plane-plastic-stress problems with axial symmetry in a simple manner, but also gave a clear picture of the octahedral shear strain and the ratio of principal stresses during loading.
- (2) The ratio of the principal stresses in such cases remained essentially constant during loading and, consequently, the deformation theory is applicable to this group of problems.
- (3) The distributions of principal strains, and octahedral shear strains, on the plastic state are less uniform than those in elastic state, although the distributions of tangential stresses appear more uniform in the plastic state. The stress concentration factor around a hole is reduced in the plastic state, but instead there is a high concentration of principal strain and of the octahedral shear strain.

(4) The ratios of the strains along the radius of their maximum value are essentially independent of the value of the maximum octahedral shear strain of the plate and the octahedral shear stress-strain curve of the material. Hence, the deformation that can be accepted by the plate before failure depends mainly on the maximum octahedral shear strain (or ductility) of the material.

(5) The stress distributions depend on the octahedral shear stress-strain curve of the material. Hence, the added load that the member can sustain between the onset of yielding and failure depends mainly upon the octahedral shear (or effective) stress-strain curve in the strain-hardening range of the material.

Lewis Flight Propulsion Laboratory,
National Advisory Committee for Aeronautics,
Cleveland, Ohio, February 28, 1950.

APPENDIX

EQUATIONS FOR ROTATING DISK AND INFINITE PLATE WITH
CIRCULAR HOLE IN ELASTIC RANGE

Rotating Disk

For a solid disk with the radial stress at the periphery ($r = b$) equal to zero, the principal stresses can be expressed in the following equations (reference 23, p. 68):

$$\left. \begin{aligned} \sigma_r &= \frac{3+\nu}{8} \rho \omega^2 (b^2 - r^2) \\ \sigma_\theta &= \frac{3+\nu}{8} \rho \omega^2 b^2 - \frac{1+3\nu}{8} \rho \omega^2 r^2 \end{aligned} \right\} \quad (39)$$

where ν is Poisson's ratio.

At $r = b$,

$$(\sigma_\theta)_b = \frac{1}{4} \rho \omega^2 b^2 (1-\nu)$$

Dividing equation (39) by $(\sigma_\theta)_b$ yields

$$\left. \begin{aligned} \frac{\sigma_r}{(\sigma_\theta)_b} &= \frac{3+\nu}{2(1-\nu)} \left[1 - \left(\frac{r}{b} \right)^2 \right] \\ \frac{\sigma_\theta}{(\sigma_\theta)_b} &= \frac{3+\nu}{2(1-\nu)} \left[1 - \frac{1+3\nu}{3+\nu} \left(\frac{r}{b} \right)^2 \right] \end{aligned} \right\} \quad (39a)$$

The stress-strain relations of plane-stress problems in the elastic range are:

$$\left. \begin{aligned} \epsilon_r &= \frac{1}{E} (\sigma_r - \nu \sigma_\theta) \\ \epsilon_\theta &= \frac{1}{E} (\sigma_\theta - \nu \sigma_r) \end{aligned} \right\} \quad (40)$$

where E is the modulus of elasticity in tension and compression.

Substituting equations (39) into equations (40) yields:

$$\left. \begin{aligned} \epsilon_r &= \frac{1}{8E} (1-\nu)(3+\nu)(\rho\omega^2 b^2) \left[1 - \frac{3(1+\nu)}{3+\nu} \left(\frac{r}{b}\right)^2 \right] \\ \epsilon_\theta &= \frac{1}{8E} (1-\nu)(3+\nu)(\rho\omega^2 b^2) \left[1 - \frac{1+\nu}{3+\nu} \left(\frac{r}{b}\right)^2 \right] \end{aligned} \right\} \quad (40a)$$

or

$$\left. \begin{aligned} \frac{\epsilon_r}{(\epsilon_\theta)_b} &= \frac{3+\nu}{2} \left[1 - \frac{3(1+\nu)}{3+\nu} \left(\frac{r}{b}\right)^2 \right] \\ \frac{\epsilon_\theta}{(\epsilon_\theta)_b} &= \frac{3+\nu}{2} \left[1 - \frac{1+\nu}{3+\nu} \left(\frac{r}{b}\right)^2 \right] \end{aligned} \right\} \quad (40b)$$

The equations for the octahedral shear stress and strain given by equations (4a), (4b), and (5a) can be applied to both the elastic and the plastic range, but equation (5b) is true only in the plastic range. The octahedral shear strain in the elastic range can be calculated by equation (4b) or simply by using the following equation:

$$\gamma = \frac{2(1+\nu)}{E} \tau = \frac{2(1+\nu)}{E} \frac{\sqrt{2}}{3} (\sigma_r^2 - \sigma_r \sigma_\theta + \sigma_\theta^2)^{1/2} \quad (41)$$

Substitute equations (39) in equations (41) to obtain:

$$\gamma = \frac{\sqrt{2}}{12E} \frac{(1+\nu)}{(3+\nu)} (\rho\omega^2 b^2) \left[(3+\nu)^2 - 4(1+\nu)(3+\nu) \left(\frac{r}{b}\right)^2 + (7+2\nu+7\nu^2) \left(\frac{r}{b}\right)^4 \right]^{1/2} \quad (41a)$$

or

$$\frac{\gamma}{\gamma_b} = \frac{1}{2(1-\nu)} \left[(3+\nu)^2 - 4(1+\nu)(3+\nu) \left(\frac{r}{b}\right)^2 + (7+2\nu+7\nu^2) \left(\frac{r}{b}\right)^4 \right]^{1/2} \quad (41b)$$

and

$\nu = 0.29$ for Inconel X (reference 24)

$\nu = 0.286$ for 16-25-6 (reference 25)

Infinite Plate With Circular Hole

For a uniformly loaded infinite plate with a circular hole, the principal stresses are (reference 23, p. 56):

$$\left. \begin{aligned} \sigma_r &= \frac{A}{r^2} + 2C \\ \sigma_\theta &= \frac{-A}{r^2} + 2C \end{aligned} \right\} \quad (42)$$

where A and C are arbitrary constants. For the case considered herein, the boundary conditions are:

$$\begin{aligned} \sigma_r &= 0 & \text{at } r &= a \\ \sigma_r &= (\sigma_r)_b & \text{at } r &= b \end{aligned}$$

These boundary conditions are used to determine the arbitrary constants A and C , which yield

$$\left. \begin{aligned} \sigma_r &= \frac{(\sigma_r)_b}{1 - \left(\frac{a}{b}\right)^2} \frac{\left(\frac{r}{a}\right)^2 - 1}{\left(\frac{r}{a}\right)^2} \\ \sigma_\theta &= \frac{(\sigma_r)_b}{1 - \left(\frac{a}{b}\right)^2} \frac{\left(\frac{r}{a}\right)^2 + 1}{\left(\frac{r}{a}\right)^2} \end{aligned} \right\} \quad (42a)$$

or

$$\left. \begin{aligned} \frac{\sigma_r}{(\sigma_\theta)_b} &= \frac{1}{1 + \left(\frac{a}{b}\right)^2} \frac{\left(\frac{r}{a}\right)^2 - 1}{\left(\frac{r}{a}\right)^2} \\ \frac{\sigma_\theta}{(\sigma_\theta)_b} &= \frac{1}{1 + \left(\frac{a}{b}\right)^2} \frac{\left(\frac{r}{a}\right)^2 + 1}{\left(\frac{r}{a}\right)^2} \end{aligned} \right\} \quad (42b)$$

Substituting equations (42a) into equations (40) yields

$$\left. \begin{aligned} \epsilon_r &= \frac{1}{E} \frac{(\sigma_r)_b}{1 - \left(\frac{a}{b}\right)^2} \frac{(1-\nu) \left(\frac{r}{a}\right)^2 - (1+\nu)}{\left(\frac{r}{a}\right)^2} \\ \epsilon_\theta &= \frac{1}{E} \frac{(\sigma_r)_b}{1 - \left(\frac{a}{b}\right)^2} \frac{(1-\nu) \left(\frac{r}{a}\right)^2 + (1+\nu)}{\left(\frac{r}{a}\right)^2} \end{aligned} \right\} \quad (43)$$

or

$$\left. \begin{aligned} \frac{\epsilon_r}{(\epsilon_\theta)_b} &= \frac{(1-\nu) \left(\frac{r}{a}\right)^2 - (1+\nu)}{\left[(1-\nu) + (1+\nu) \left(\frac{a}{b}\right)^2 \right] \left(\frac{r}{a}\right)^2} \\ \frac{\epsilon_\theta}{(\epsilon_\theta)_b} &= \frac{(1-\nu) \left(\frac{r}{a}\right)^2 + (1+\nu)}{\left[(1-\nu) + (1+\nu) \left(\frac{a}{b}\right)^2 \right] \left(\frac{r}{a}\right)^2} \end{aligned} \right\} \quad (43a)$$

Substituting equations (42a) into equation (41) yields

$$\gamma = \frac{2\sqrt{2}(1+\nu)}{3E} \frac{(\sigma_r)_b}{1 - \left(\frac{a}{b}\right)^2} \left[\frac{\left(\frac{r}{a}\right)^4 + 3}{\left(\frac{r}{a}\right)^4} \right]^{1/2} \quad (44)$$

or

$$\frac{\gamma}{\gamma_b} = \left\{ \frac{\left(\frac{r}{a}\right)^4 + 3}{\left[1 + 3\left(\frac{a}{b}\right)^4\right]\left(\frac{r}{a}\right)^4} \right\}^{1/2}$$

REFERENCES

1. Nadai, A.: Plasticity. McGraw-Hill Book Co., Inc., 1931.
2. Nadai, A., and Donnell, L. H.: Stress Distribution in Rotating Disks of Ductile Material after the Yield Point Has Been Reached. Trans. A.S.M.E., vol. 51, pt. I, APM-51-16, 1929, pp. 173-180; discussion, pp. 180-181.
3. Gleyzal, A.: Plastic Deformation of a Circular Diaphragm under Pressure. Jour. Appl. Mech., vol. 15, no. 3, Sept. 1948, pp. 288-296.
4. Millenson, M. B., and Manson, S. S.: Determination of Stresses in Gas-Turbine Disks Subjected to Plastic Flow and Creep. NACA Rep. 906, 1948. (Formerly NACA TN 1636.)
5. MacGregor, C. W., and Tierney, W. D.: Developments in High-Speed Rotating Disk Research at M.I.T. Welding Jour. Suppl., vol. 27, no. 6, June 1948, pp. 303S-309S.
6. Holms, Arthur G., and Jenkins, Joseph E.: Effect of Strength and Ductility on Burst Characteristics of Rotating Disks. NACA TN 1667, 1948.
7. Hencky, Heinrich: Zur Theorie plastischer Deformationen und der hierdurch im Material hervorgerufenen Nachspannungen. Z.f.a.M.M., Bd. 4, Heft 4, Aug. 1924, S. 323-334.

8. Nadai, A.: Theories of Strength. Trans. A.S.M.E., vol. 55, APM-55-15, 1933, pp. 111-129.
9. Nadai, A.: Plastic Behavior of Metals in the Strain-Hardening Range. Part I. Jour. Appl. Phys., vol. 8, no. 3, March 1937, pp. 205-213.
10. Ilyushin, A.A.: Relation between the Theory of Saint Venant-Levy-Mises and the Theory of Small Elastic-Plastic Deformations. RMB-1, trans. by Appl. Math. Group, Brown Univ., for David W. Taylor Model Basin (Washington, D.C.), 1945.
11. Ilyushin, A. A.: The Theory for Small Elastic-Plastic Deformations. RMB-17, trans. by Grad. Div. Appl. Math., Brown Univ., for David W. Taylor Model Basin (Washington, D.C.), 1947. (Contract NObs-34166.)
12. Prager, W.: Strain Hardening under Combined Stresses. Jour. Appl. Phys., vol. 16, no. 12, Dec. 1945, pp. 837-840.
13. Drucker, D. C.: A Reconsideration of Deformation Theories of Plasticity. Trans. A.S.M.E., vol. 71, no. 5, July 1949, pp 587-592.
14. Lessells, J. M., and MacGregor, C. W.: Combined Stress Experiments on a Nickel-Chrome-Molybdenum Steel. Jour. Franklin Inst., vol. 230, no. 2, Aug. 1940, pp. 163-181.
15. Osgood, W. R.: Combined-Stress Tests on 24S-T Aluminum Alloy Tubes. Jour. Appl. Mech., vol. 14, no. 2, June 1947, pp. A147-A153.
16. Fraenkel, S. J.: Experimental Studies of Biaxially Stressed Mild Steel in the Plastic Range. Jour. Appl. Mech., vol. 15, no. 3, Sept. 1948, pp. 193-200.
17. Davis, H. E., and Parker, E. R.: Behavior of Steel under Biaxial Stress as Determined by Tests on Tubes. Jour. Appl. Mech., vol. 15, no. 3, Sept. 1948, pp. 201-215.
18. Lankford, W. T., Low, J. R., and Gensemer, M.: The Plastic Flow of Aluminum Alloy Sheet under Combined Loads. Trans. A.I.M.E., Inst. Metals Div., vol. 171, 1947, pp. 574-604.
19. Bickley, W. G.: Formulae for Numerical Integration. The Math. Gazette, vol. XXIII, no. 256, Oct. 1939, pp. 352-359.
20. Milne, William Edmund: Numerical Calculus. Princeton Univ. Press, 1949.

- 1383
21. Griffith, George E.: Experimental Investigation of the Effects of Plastic Flow in a Tension Panel with a Circular Hole. NACA TN 1705, 1948.
 22. Stowell, Elbridge Z.: Stress and Strain Concentration at a Circular Hole in an Infinite Plate. NACA TN 2073, 1950.
 23. Timoshenko, S.: Theory of Elasticity. McGraw-Hill Book Co., Inc., 1934.
 24. Anon.: Nickel and Nickel Alloys. The International Nickel Co., Inc. (New York), 1947.
 25. Fleischmann, Martin: 16-25-6 Alloy for Gas Turbines. Iron Age, vol. 157, no. 3, Jan 17, 1946, pp. 44-53; cont., vol. 157, no. 4, Jan. 24, 1946, pp. 50-60.

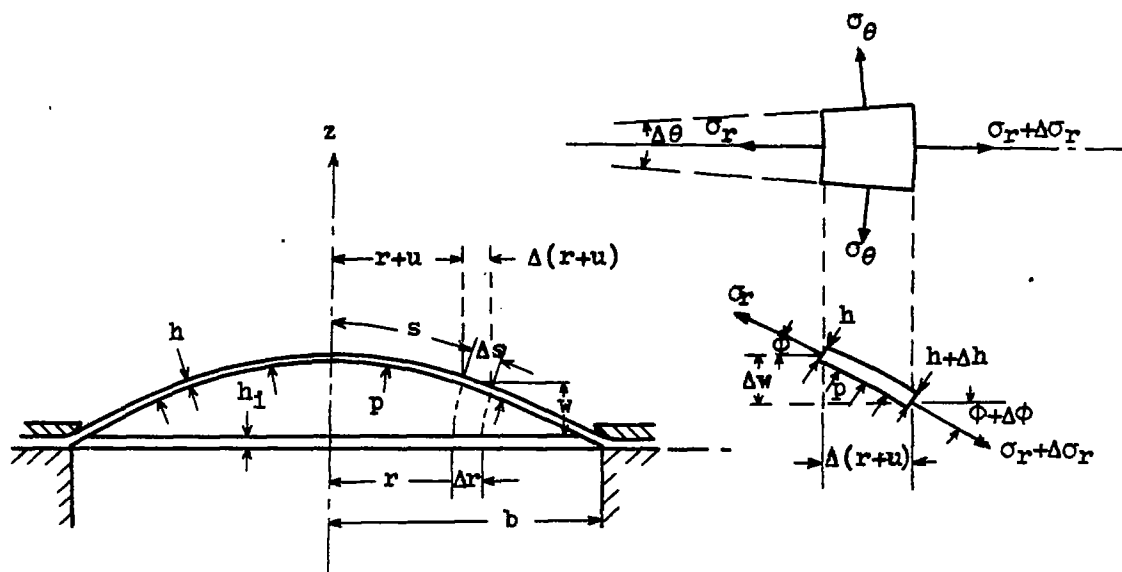


Figure 1. - Thin circular membrane (under pressure) and its element.

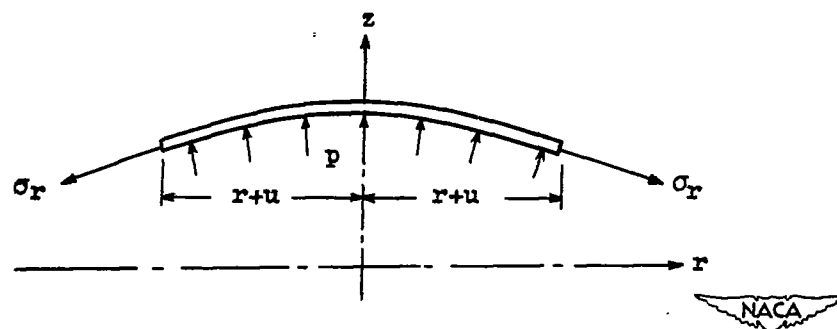


Figure 2. - Cap of membrane with radius $r+u$.

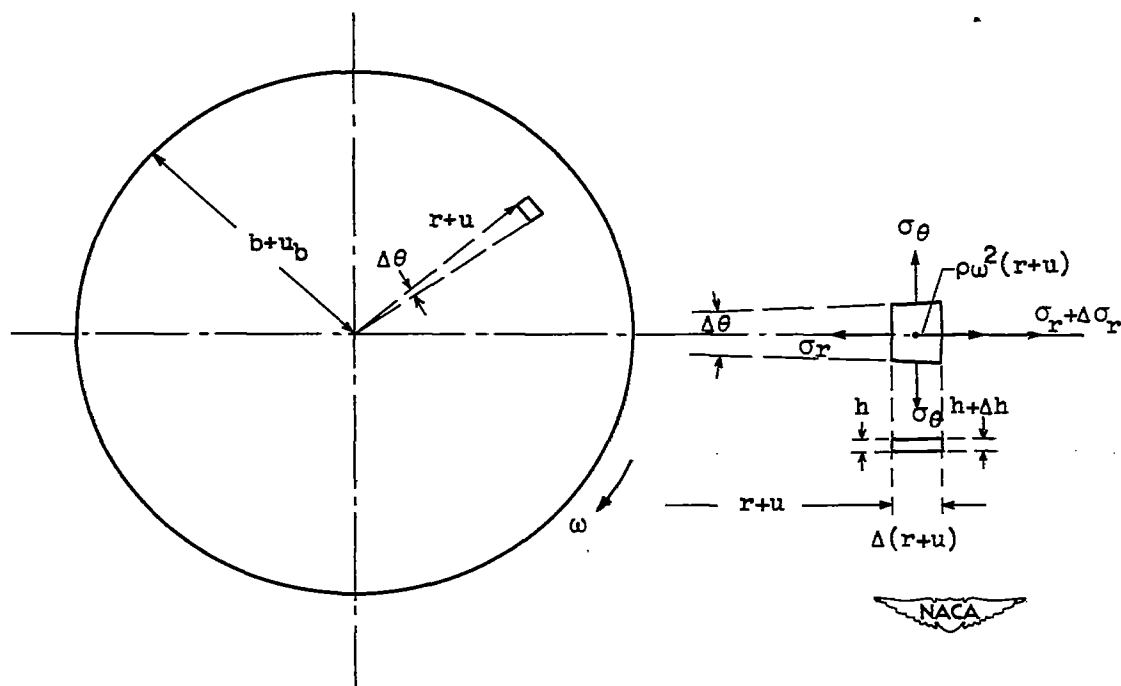
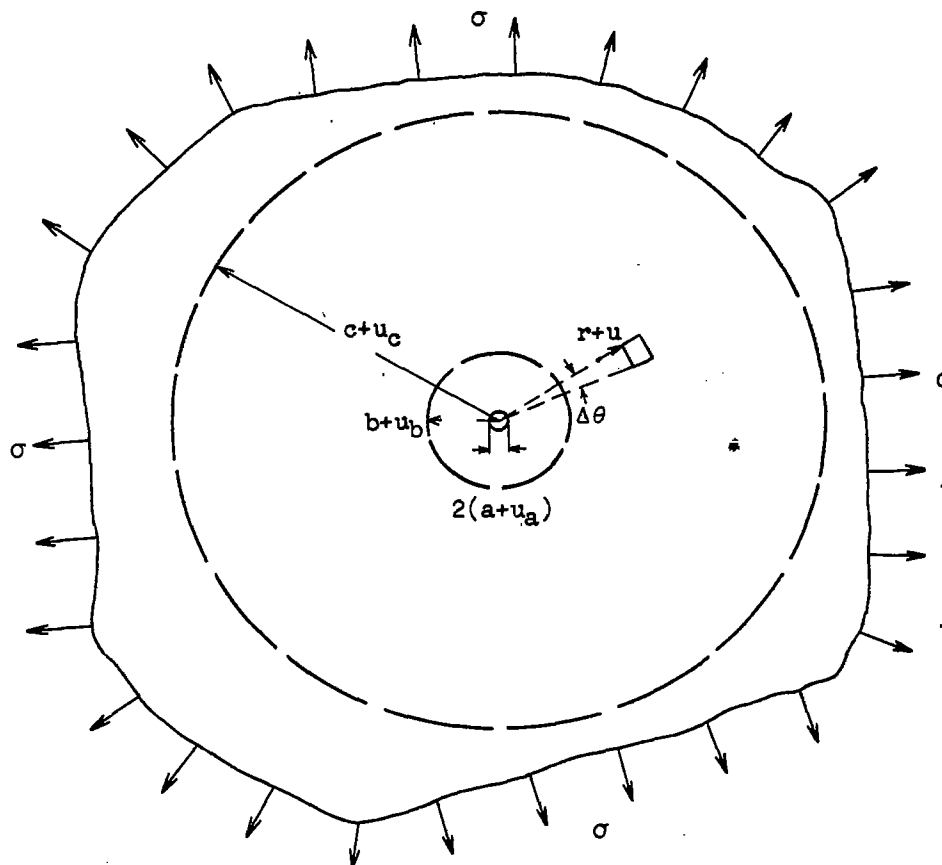
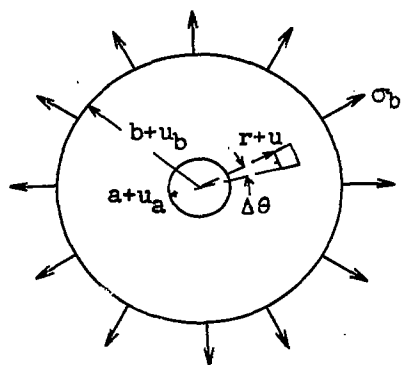


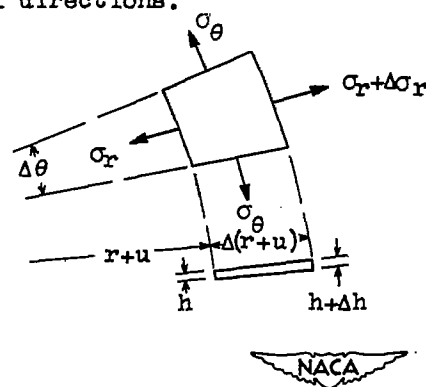
Figure 3. - Rotating disk and its element.



(a) Infinite plate with circular hole uniformly stressed in its plane in all directions.



(b) Flat ring radially stressed.



(c) Element.

Figure 4. - Infinite plate with circular hole, flat ring radially stressed and its element.

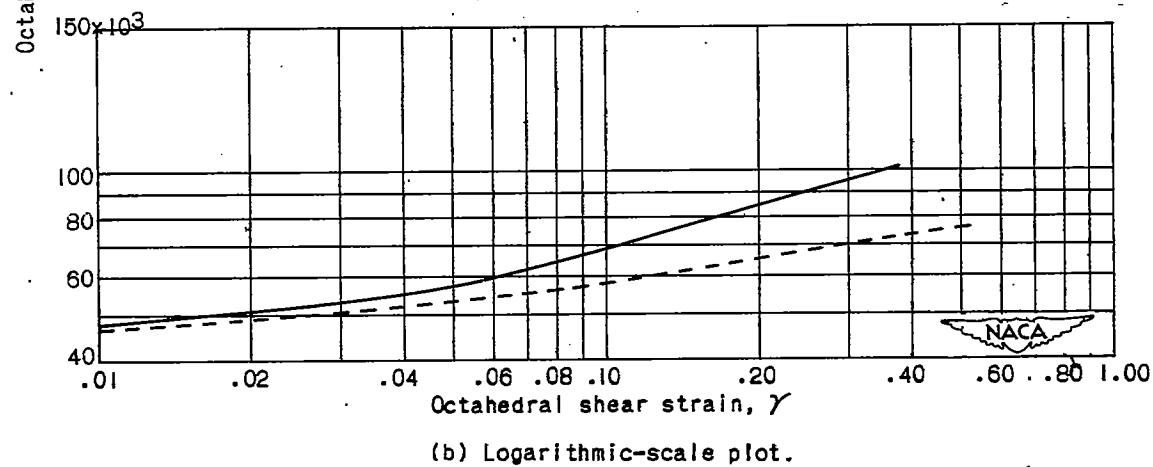
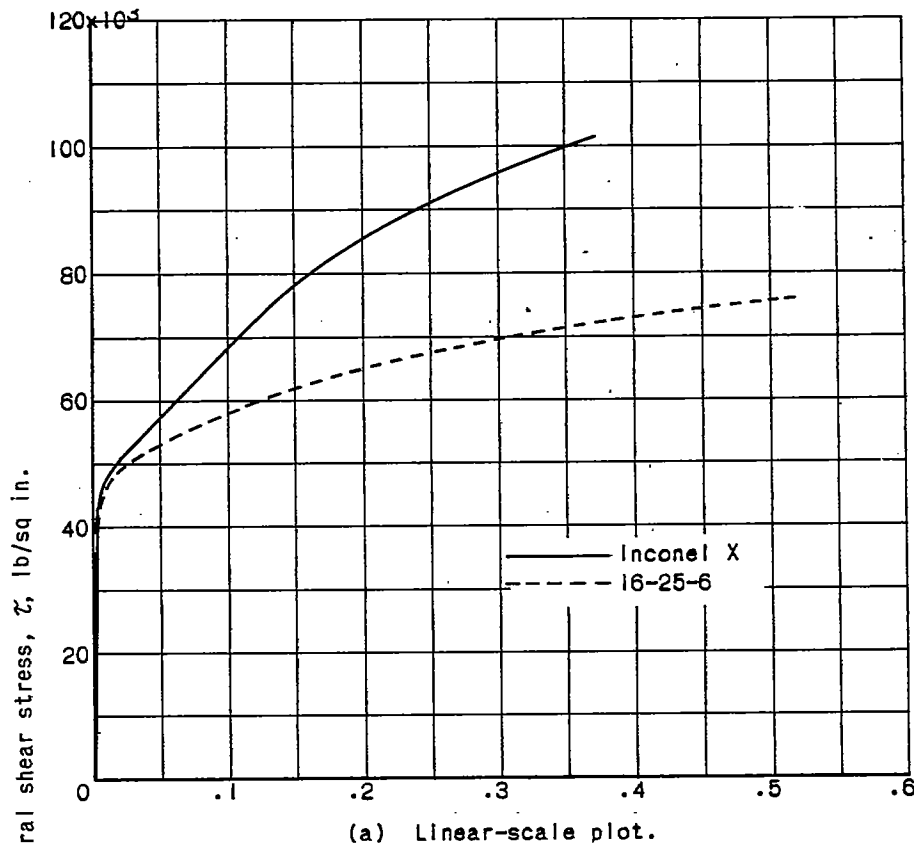


Figure 5. - True octahedral shear stress-strain curves.

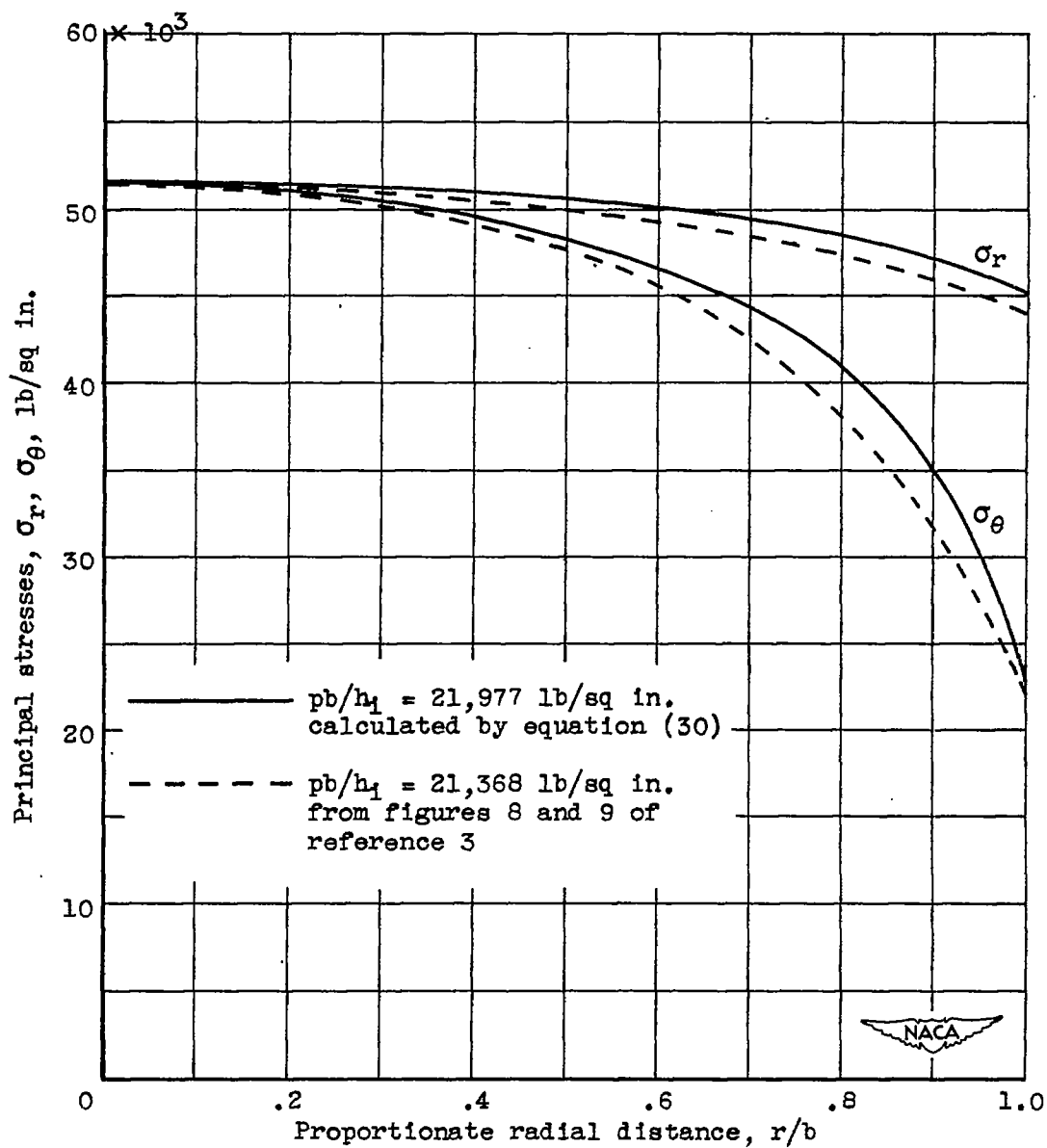
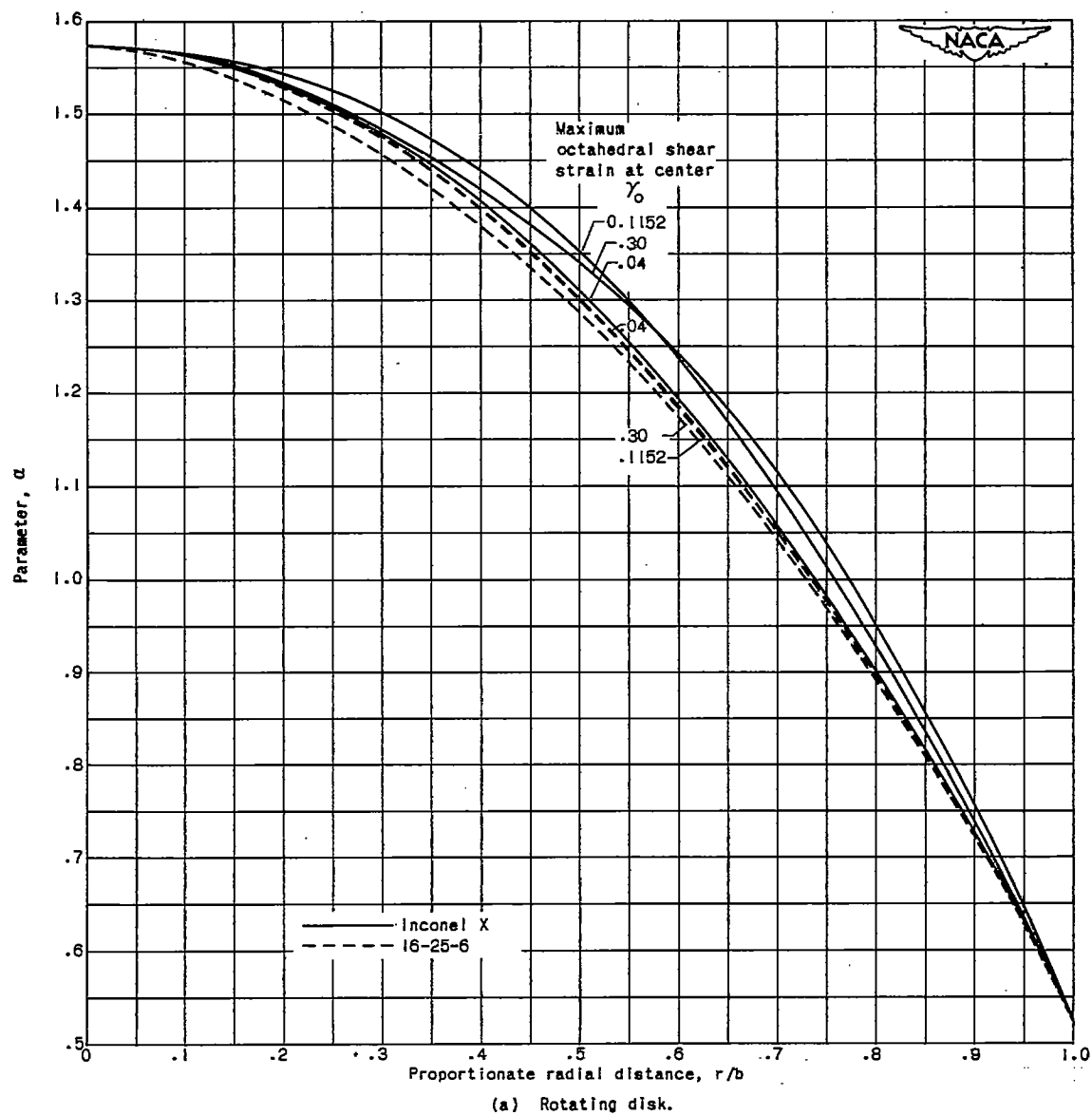


Figure 6. - Variation of radial and circumferential stresses σ_r and σ_θ with proportionate radius.

Figure 7. - Variations of parameter α with proportionate radius for Inconel X and 16-25-6.

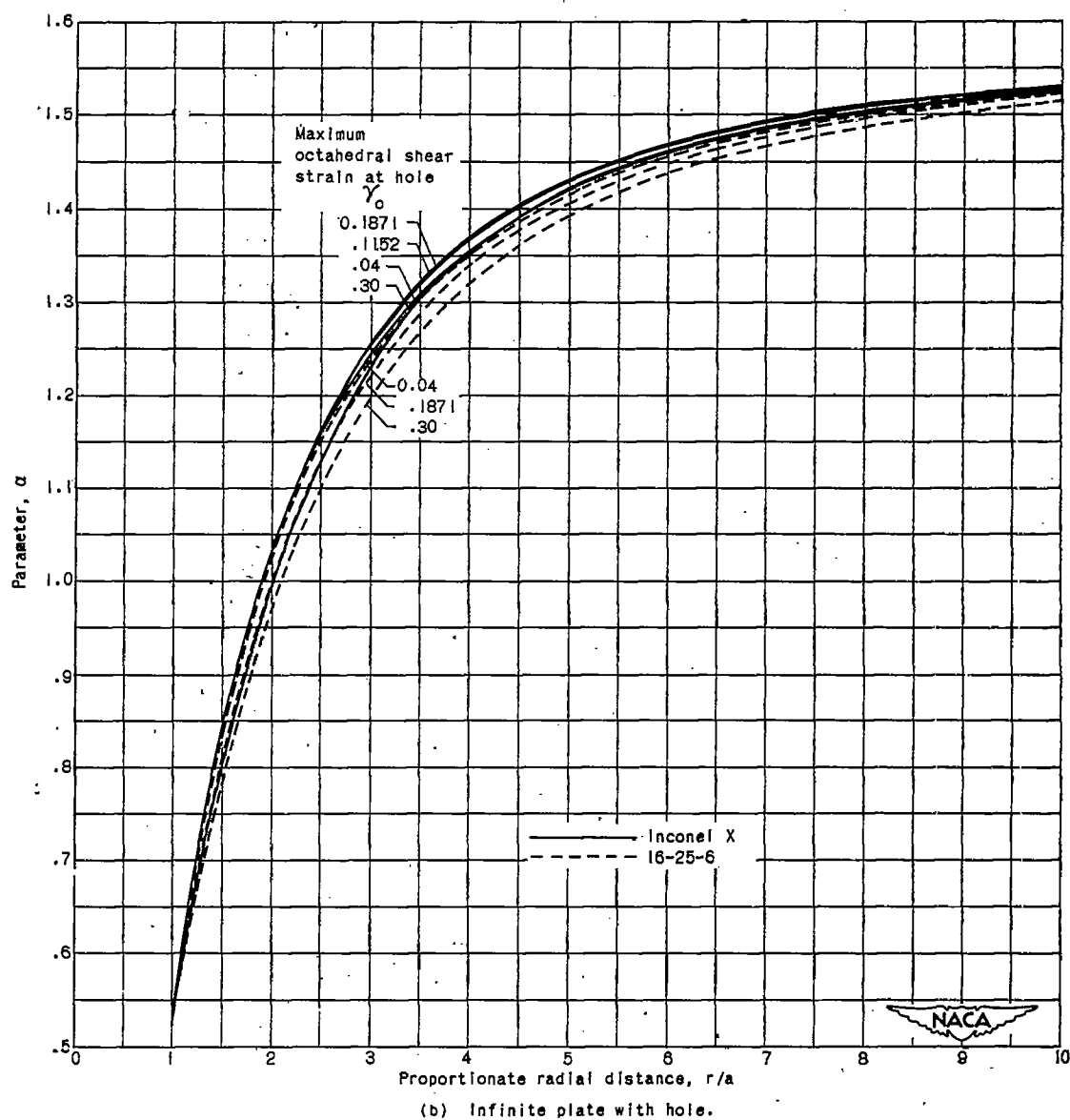
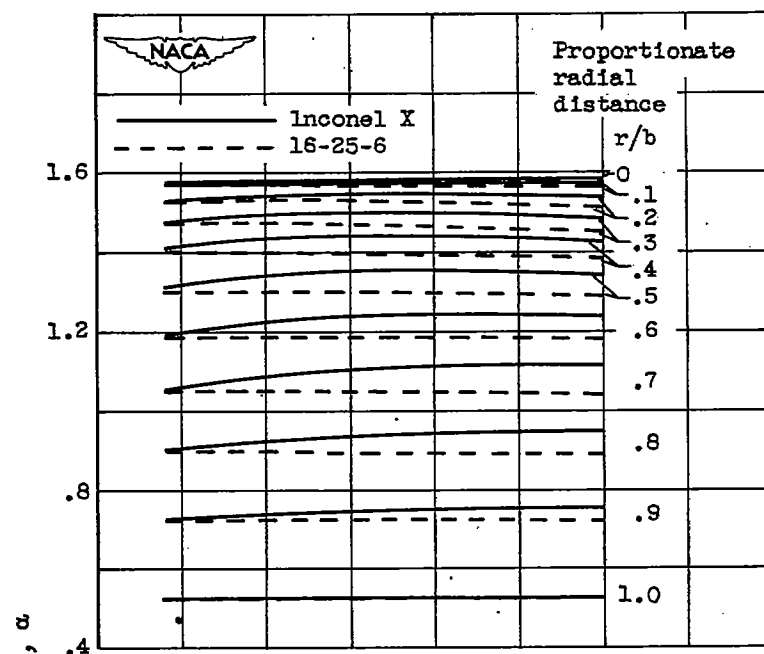
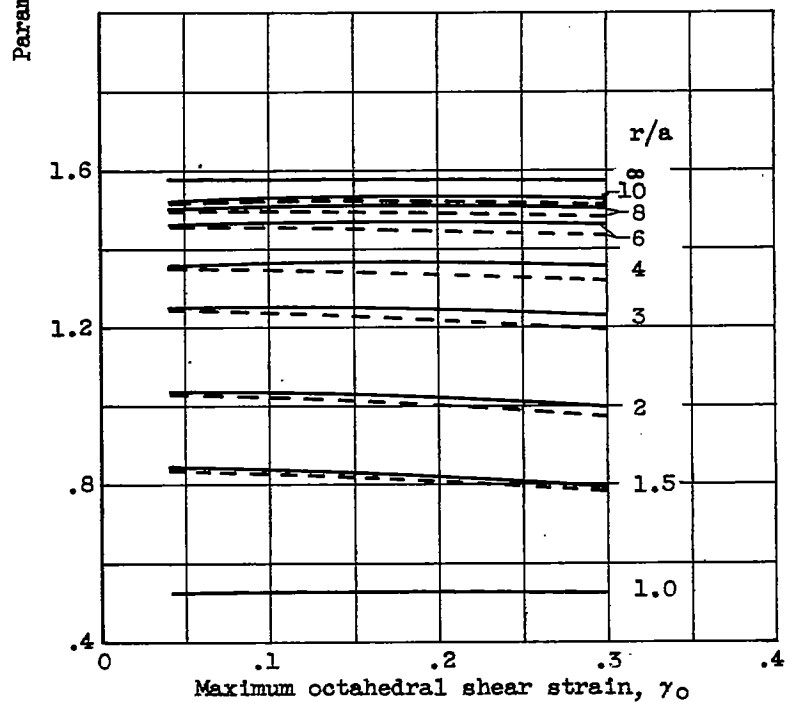


Figure 7. - Concluded. Variations of parameter α with proportionate radius for Inconel X and 16-25-6.



(a) Rotating disk.



(b) Infinite plate with hole.

Figure 8. - Variation of parameter α with maximum octahedral shear strain at different radii.

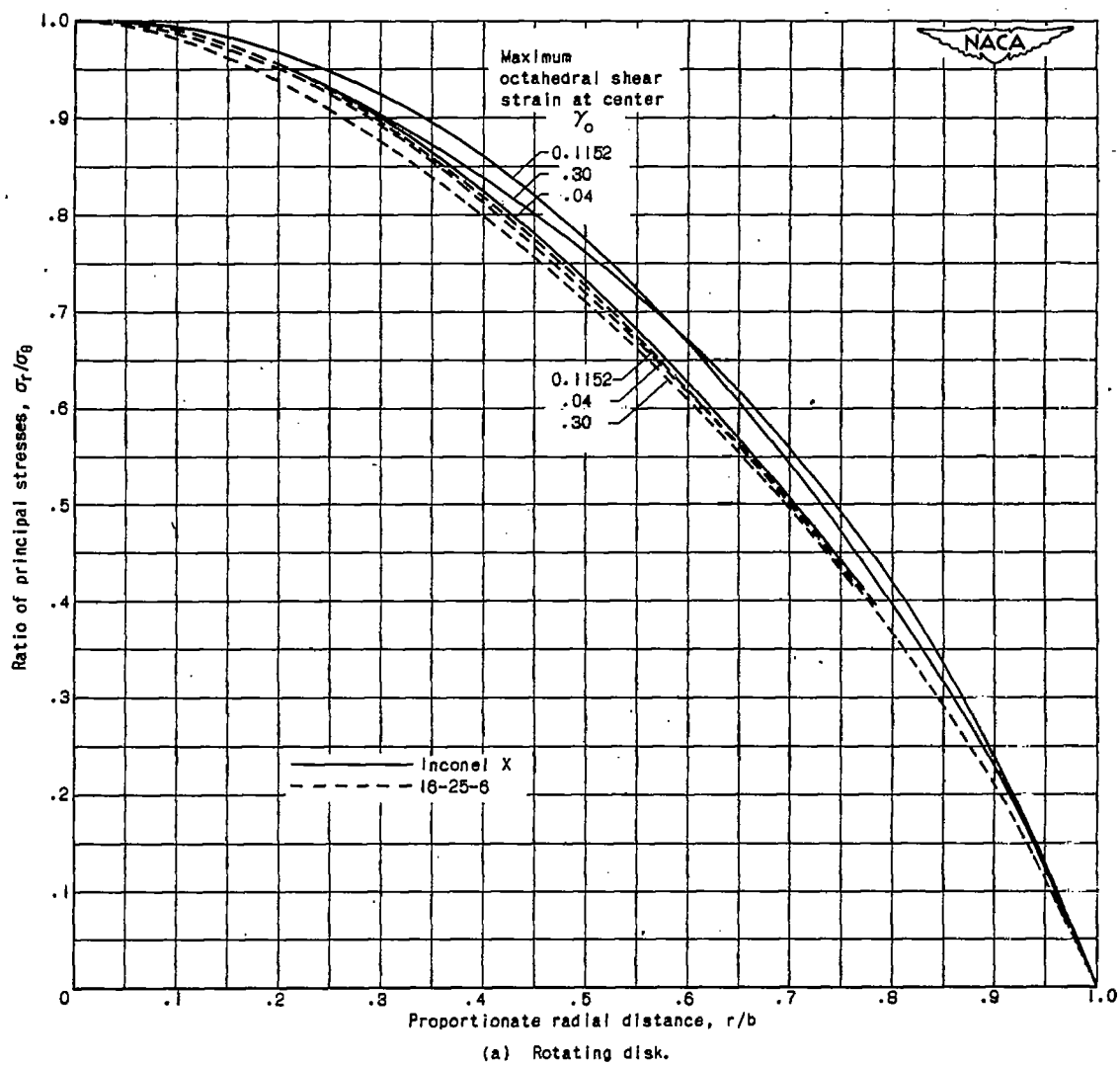


Figure 9. - Variations of ratio of principal stresses with proportionate radial distance.

1383

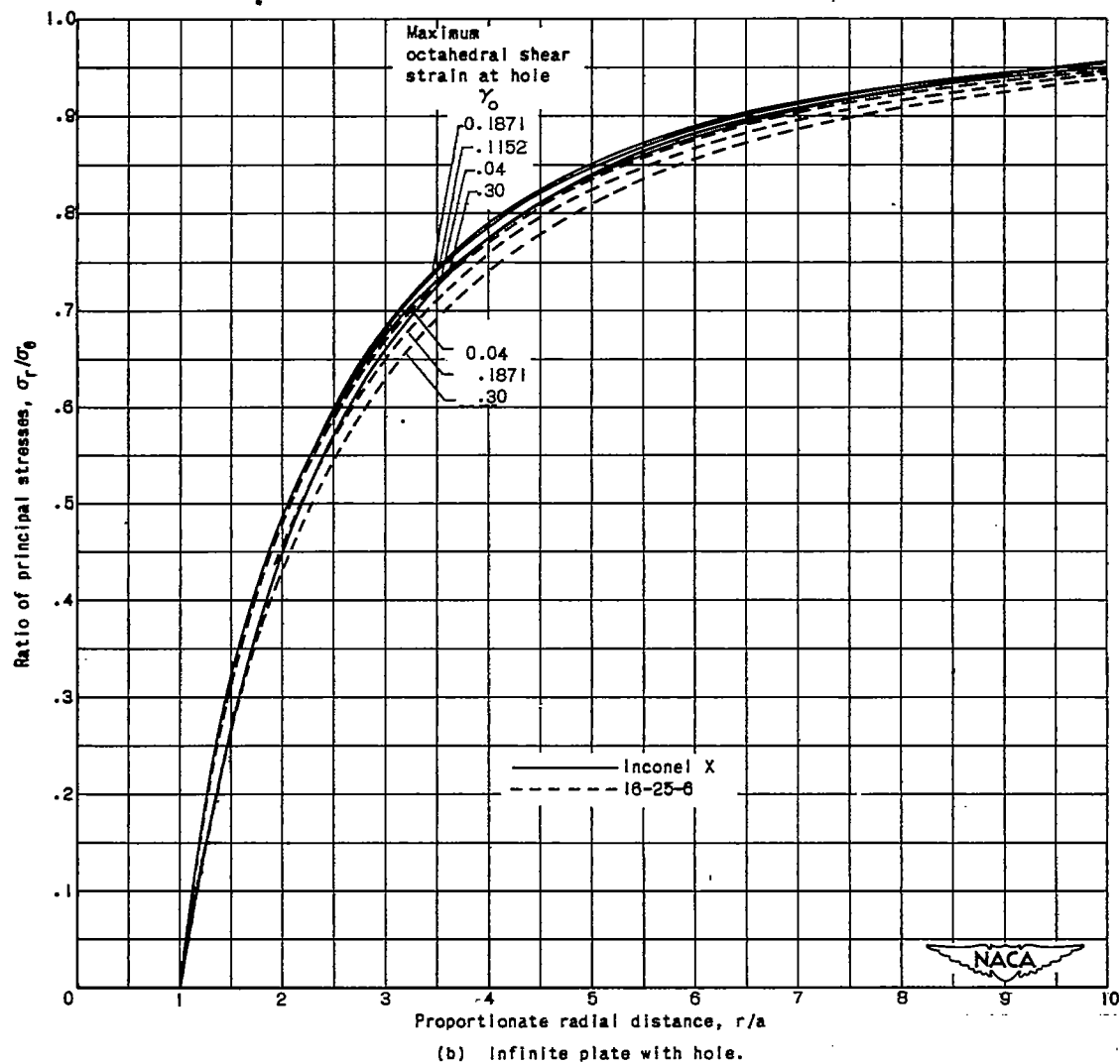


Figure 8. - Continued. Variations of ratio of principal stresses with proportionate radial distance.

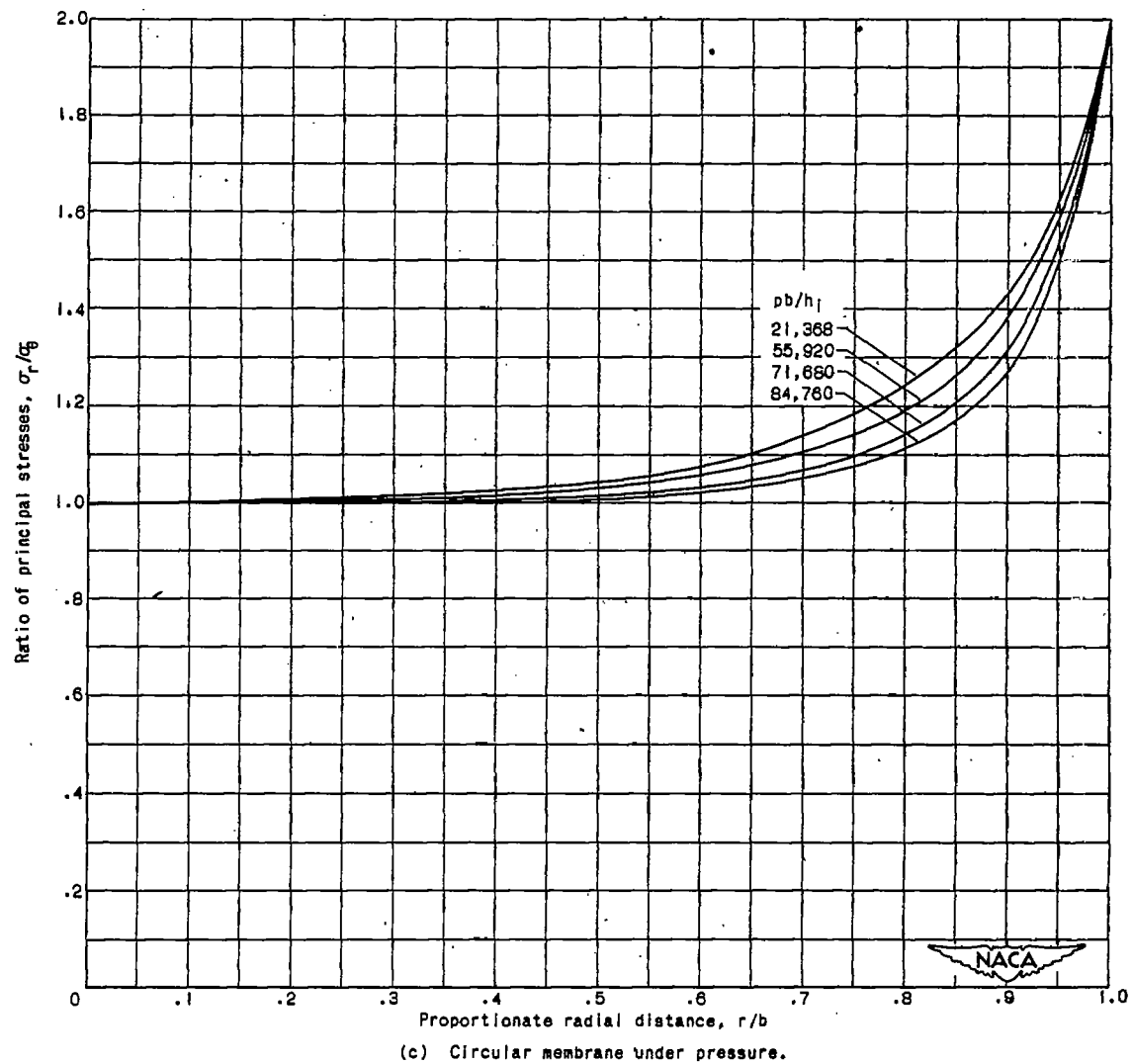


Figure 9. - Concluded. Variations of ratio of principal stresses with proportionate radial distance.

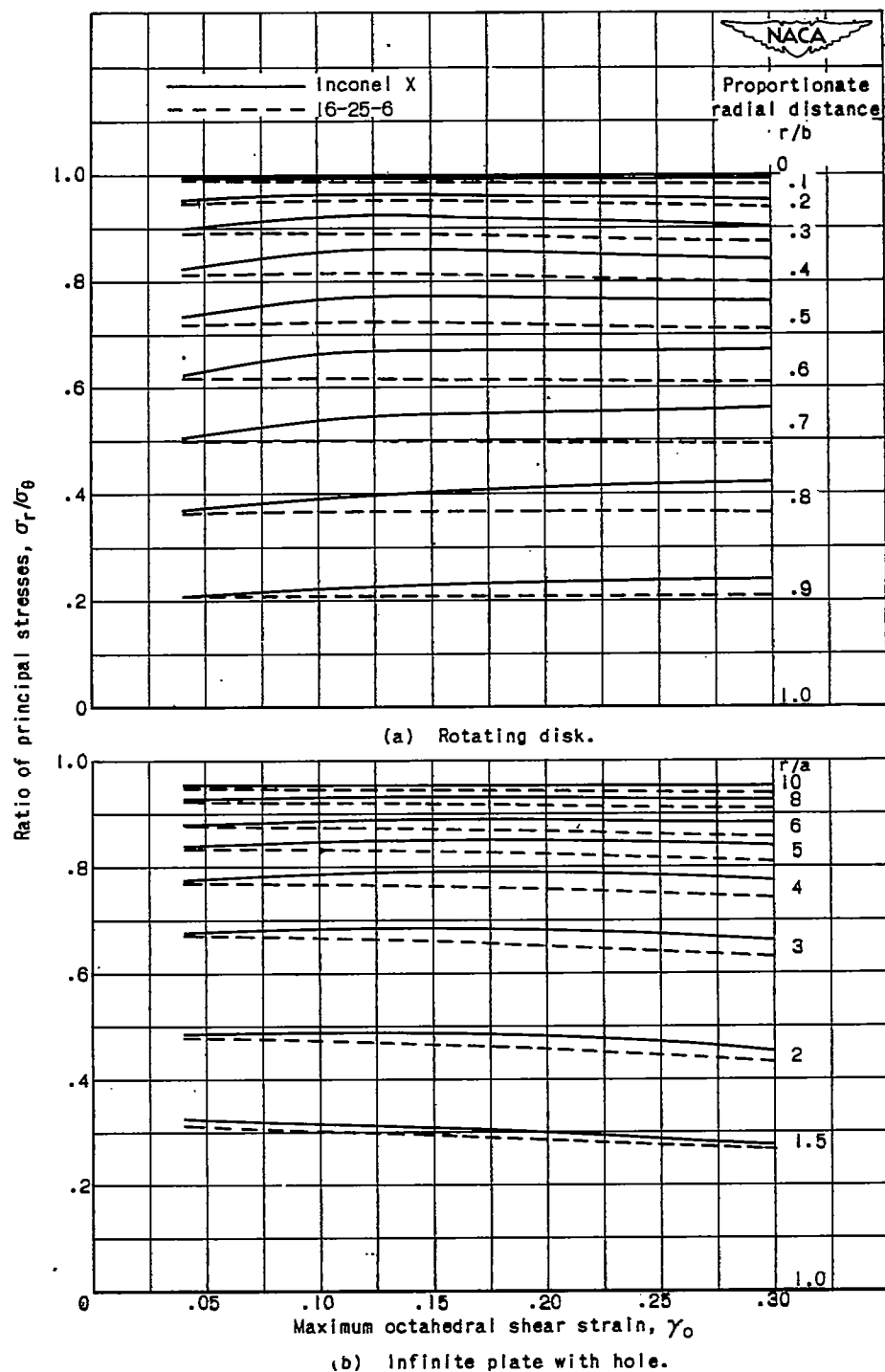
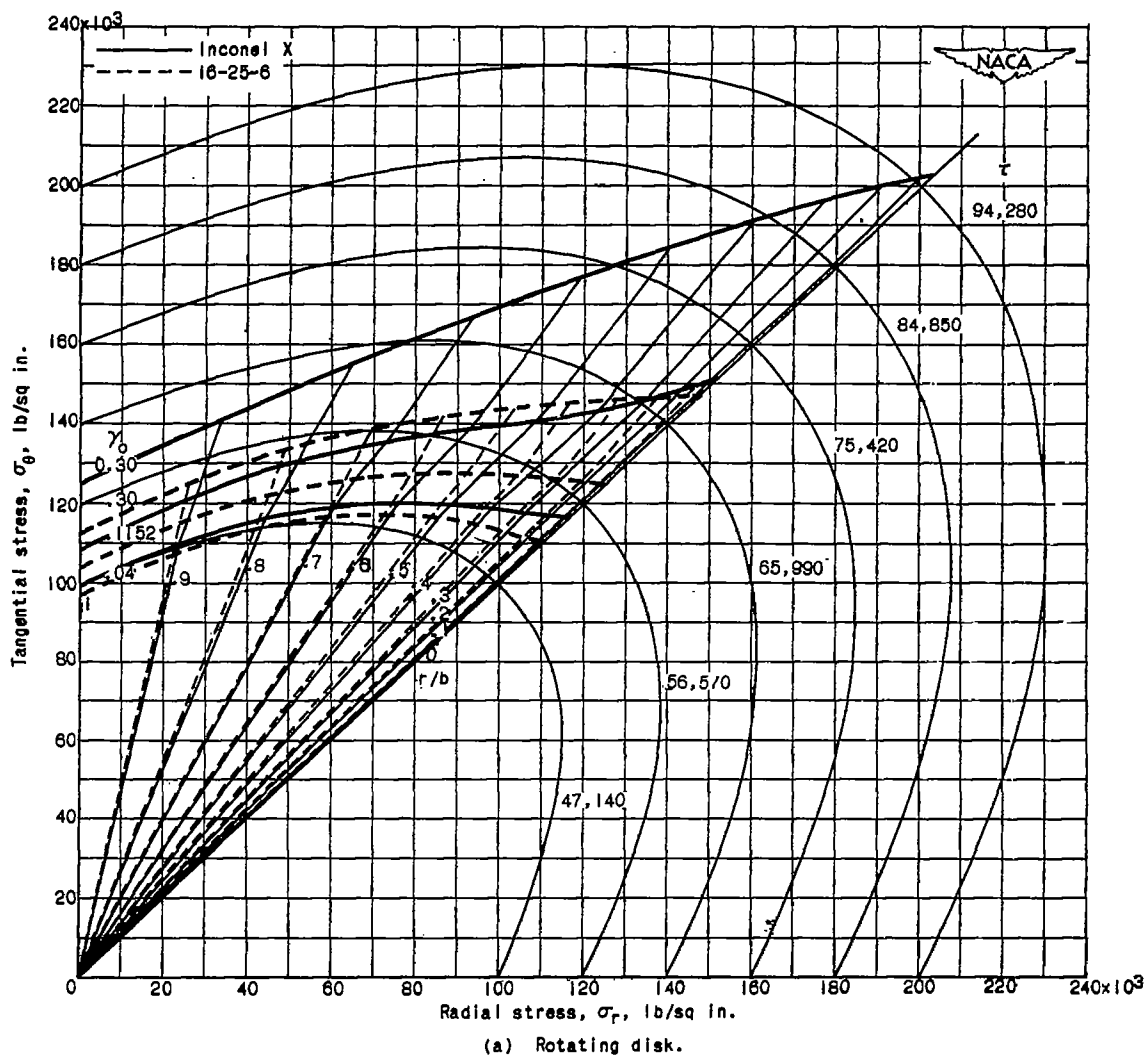


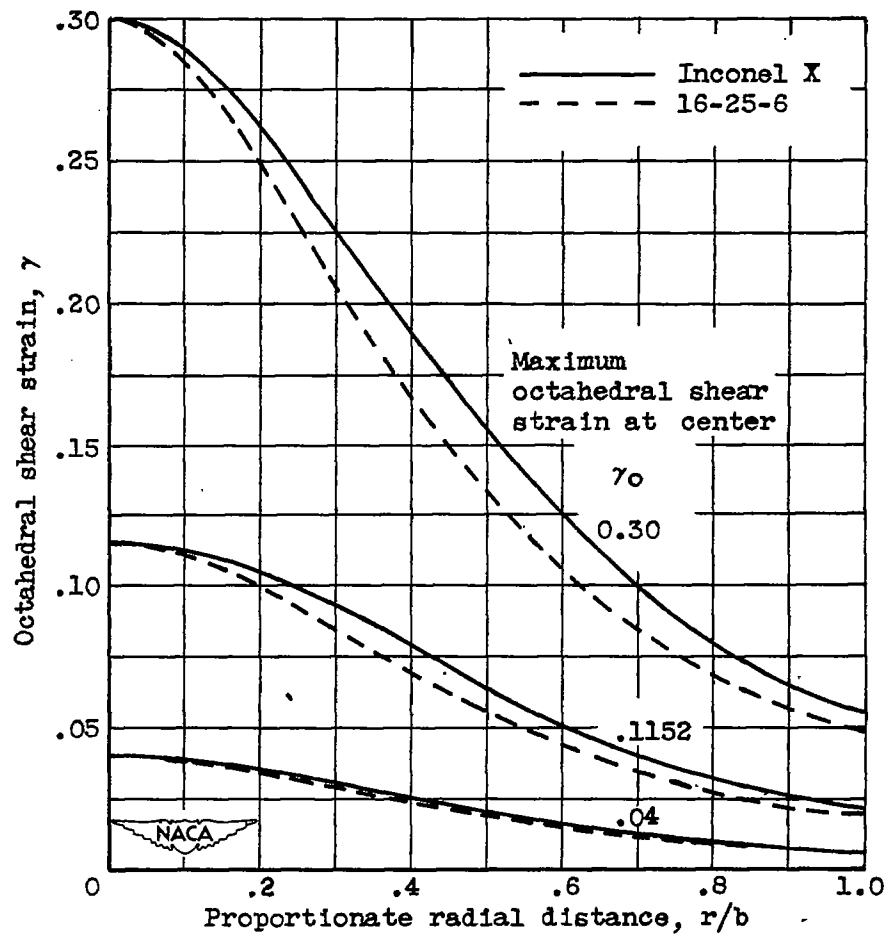
Figure 10. - Variation of ratio of principal stresses σ_r/σ_θ with maximum octahedral shear strain γ_o at different radii.





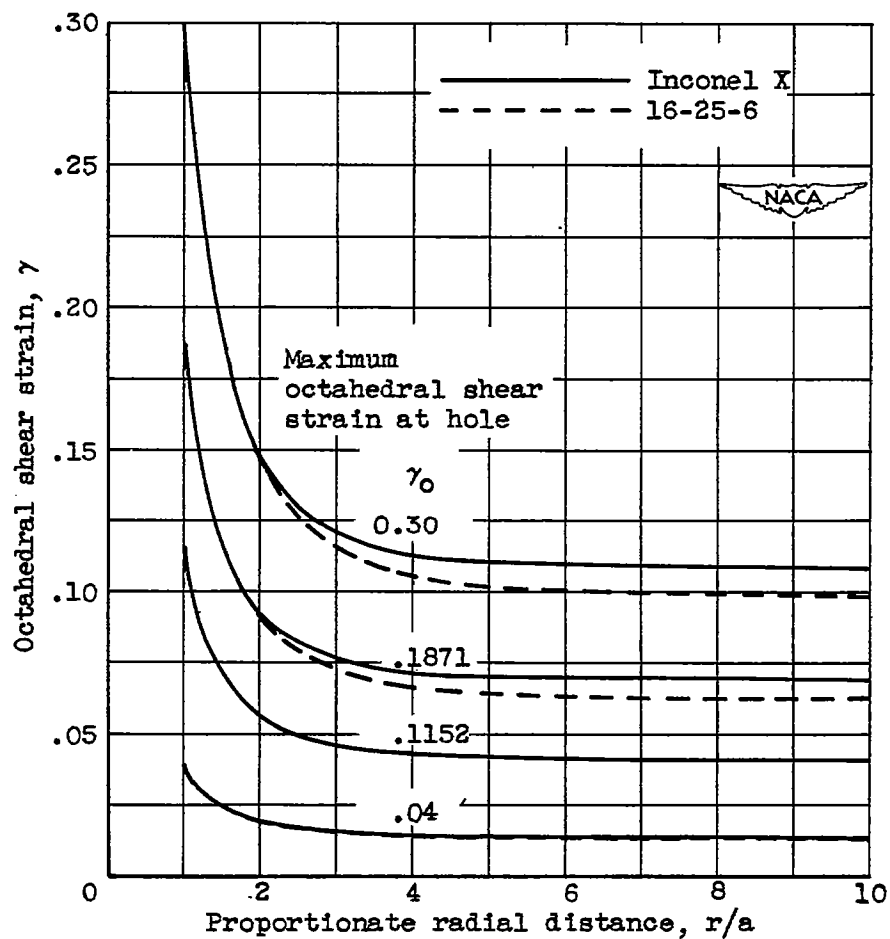
1383

1383



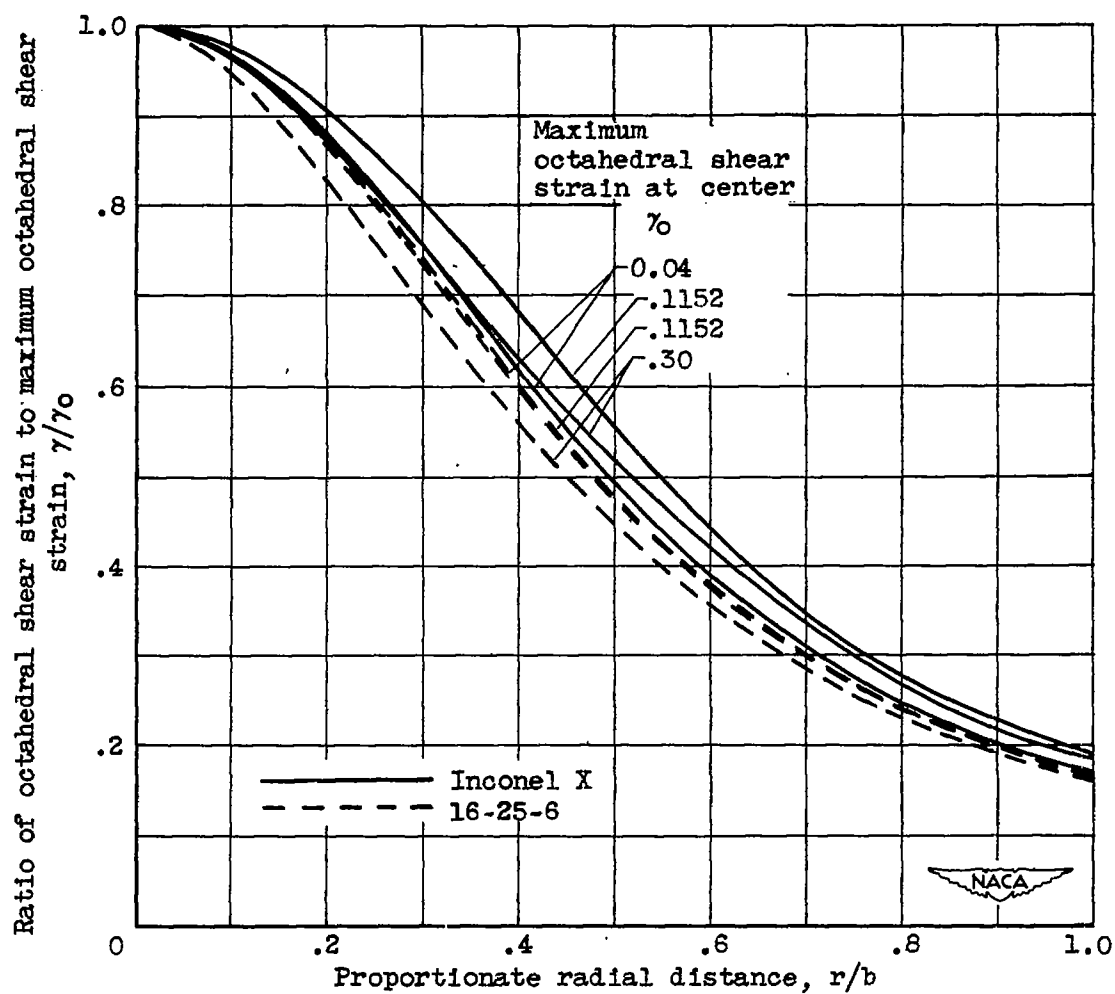
(a) Rotating disk.

Figure 12. - Variation of octahedral shear strain with proportionate radial distance.



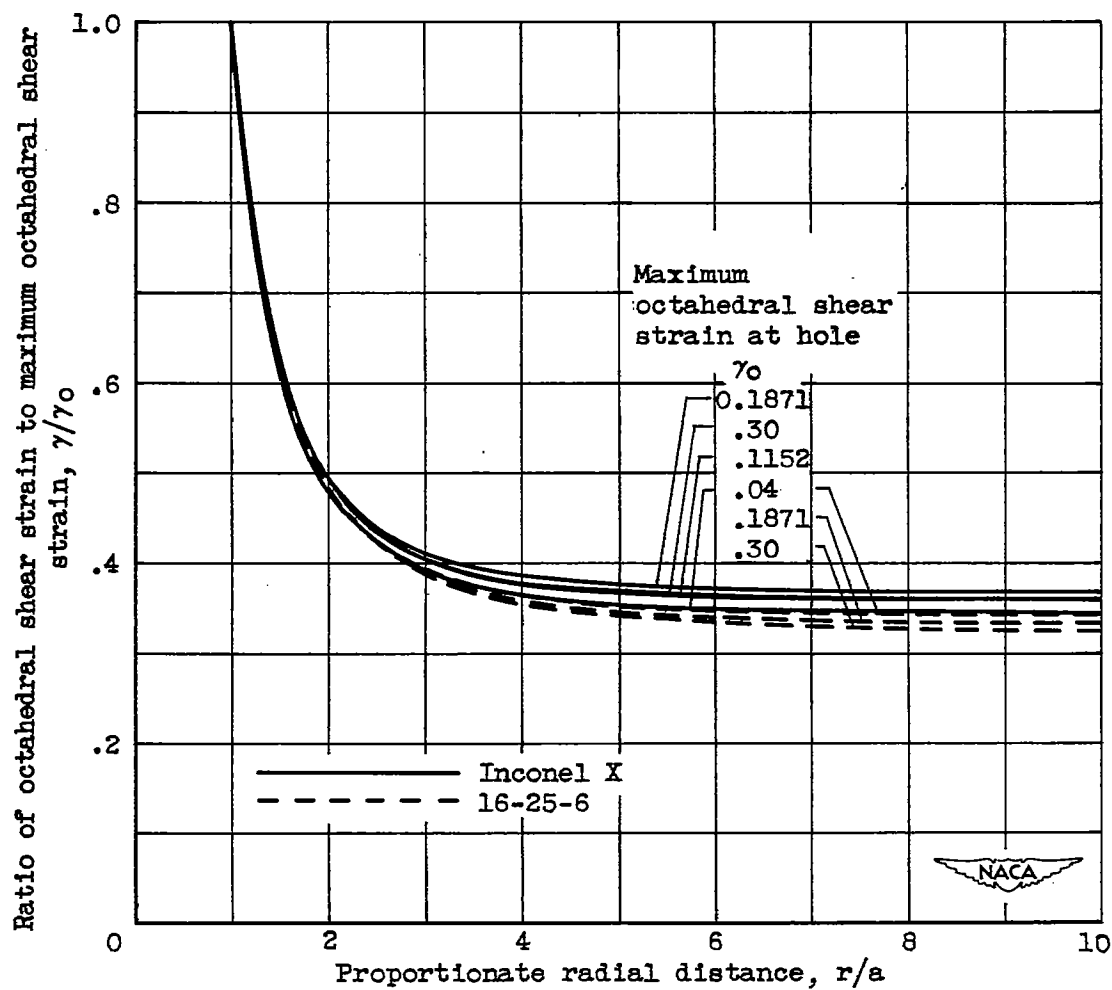
(b) Infinite plate with hole.

Figure 12. - Concluded. Variation of octahedral shear strain with proportionate radial distance.



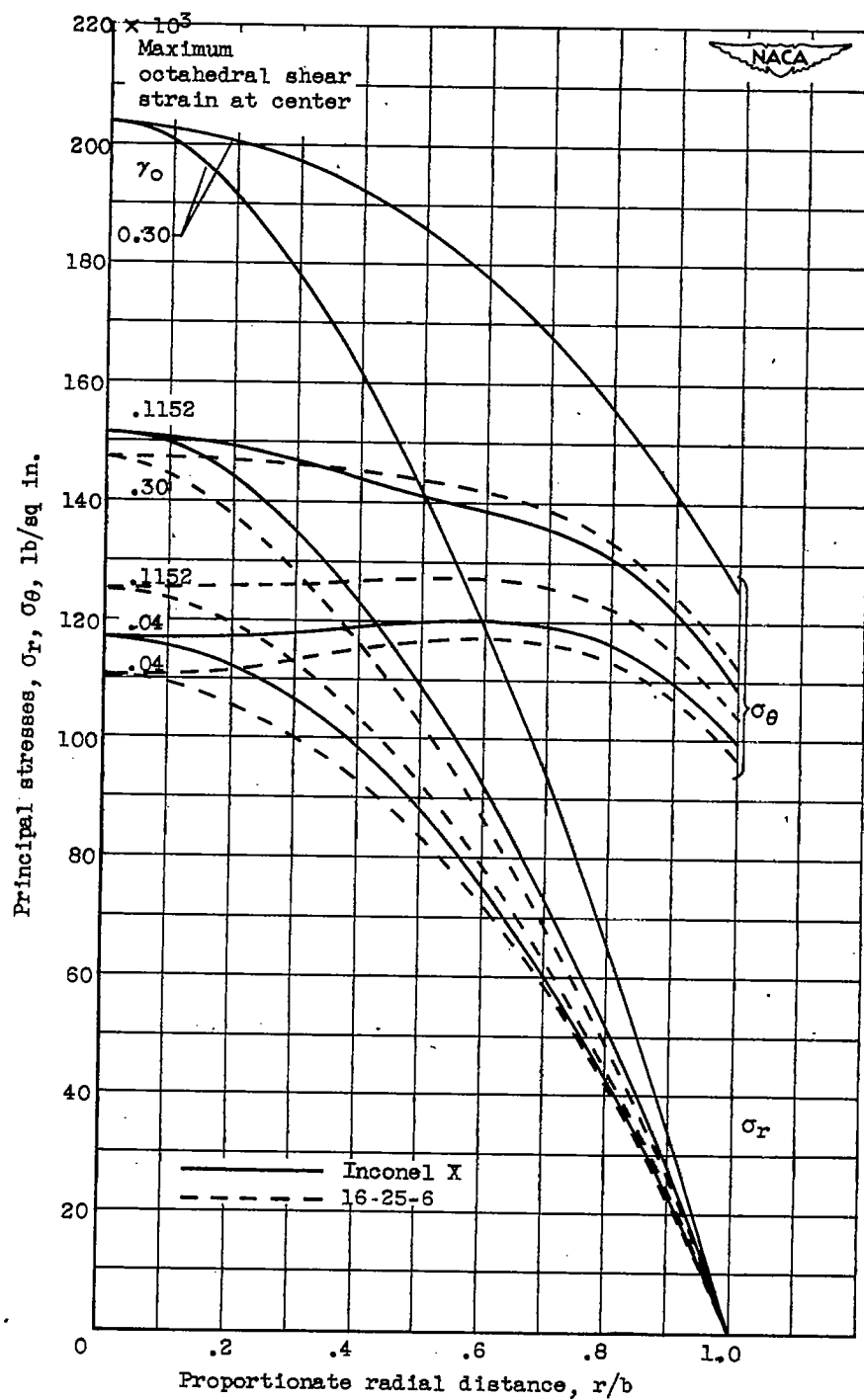
(a) Rotating disk.

Figure 13. - Variation of ratio of octahedral shear strain with proportionate radial distance.



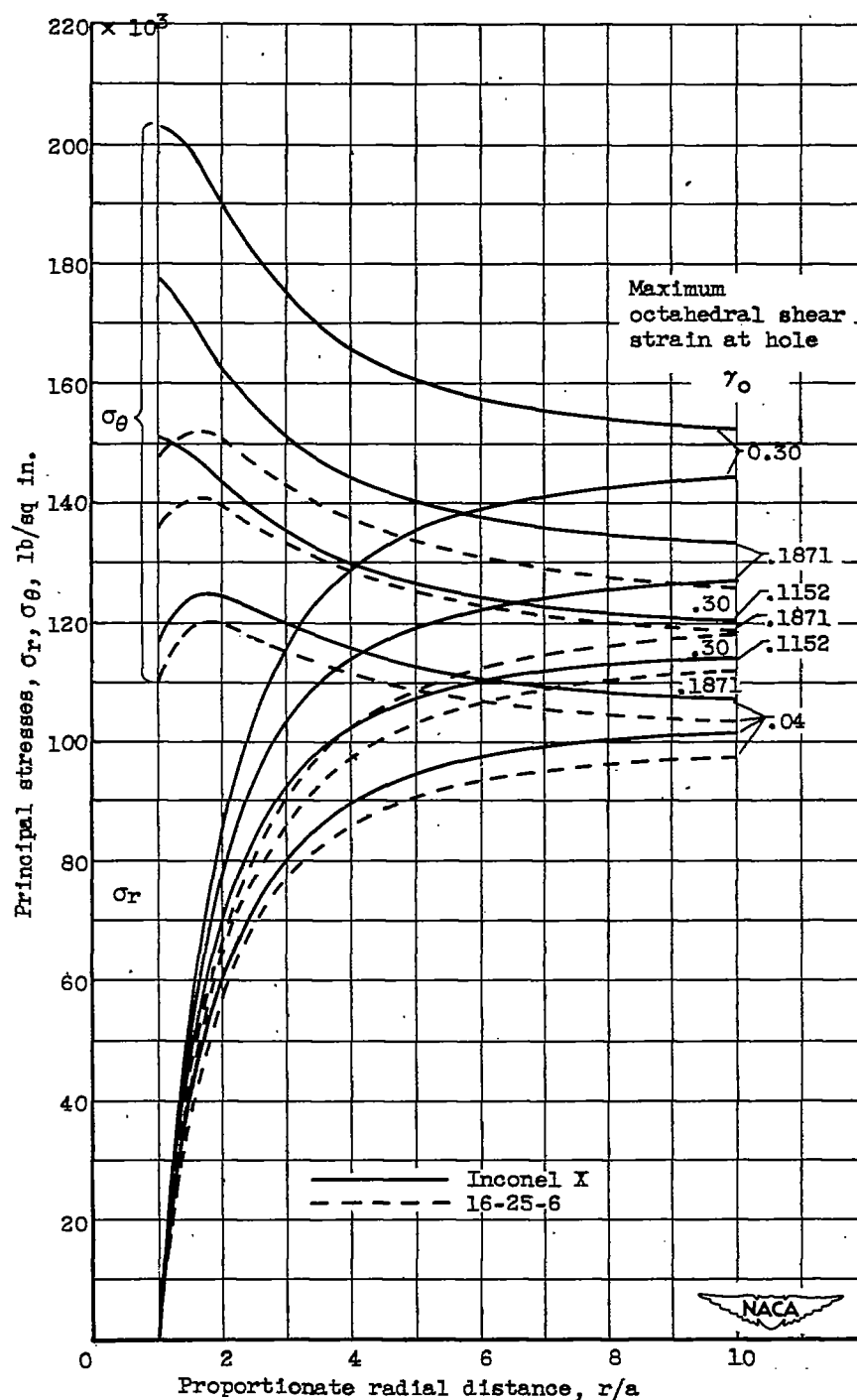
(b) Infinite plate with hole.

Figure 13. - Concluded. Variation of ratio of octahedral shear strain with proportionate radial distance.



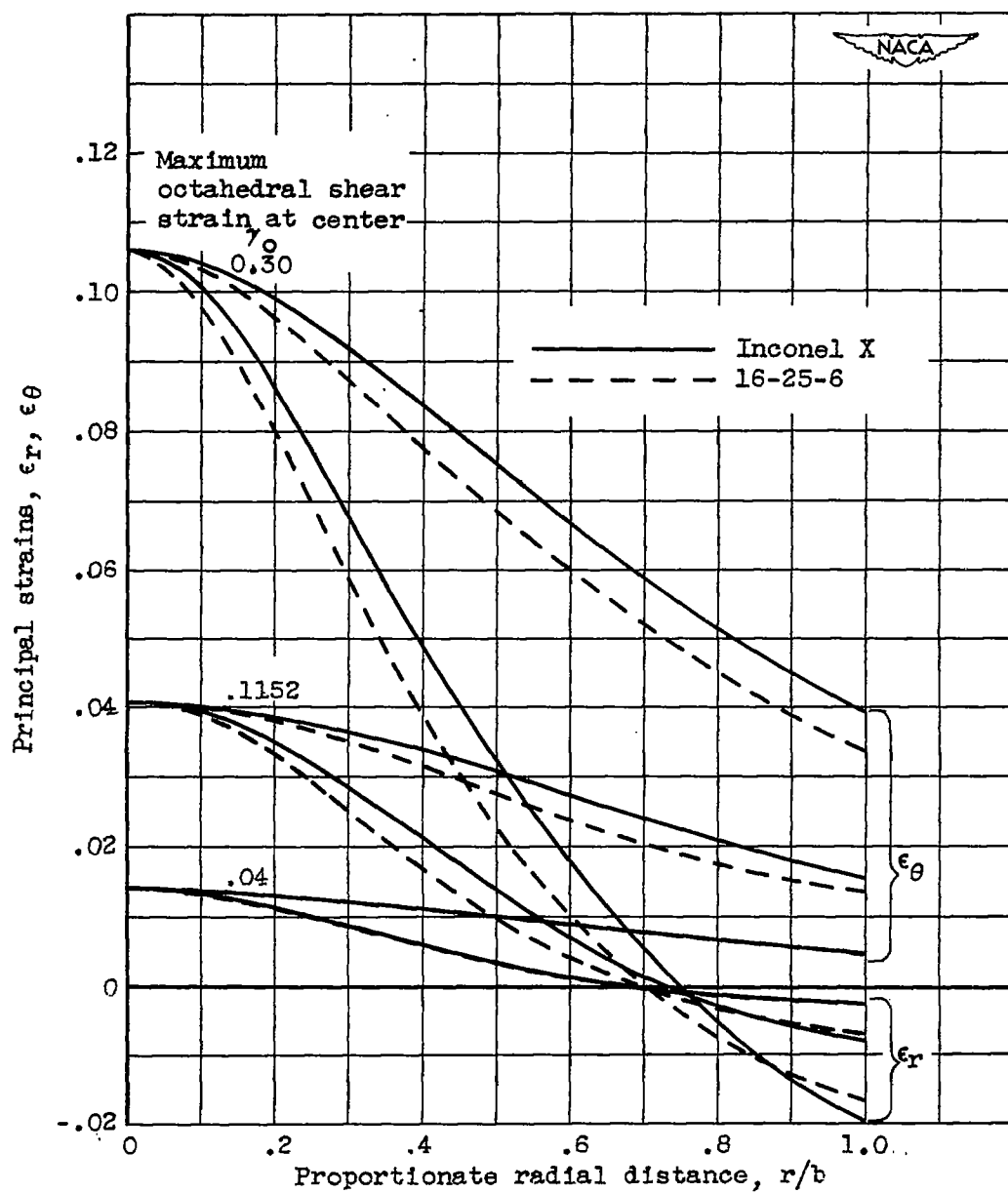
(a) Rotating disk.

Figure 14. - Variation of principal stresses σ_r and σ_θ with proportionate radial distance.



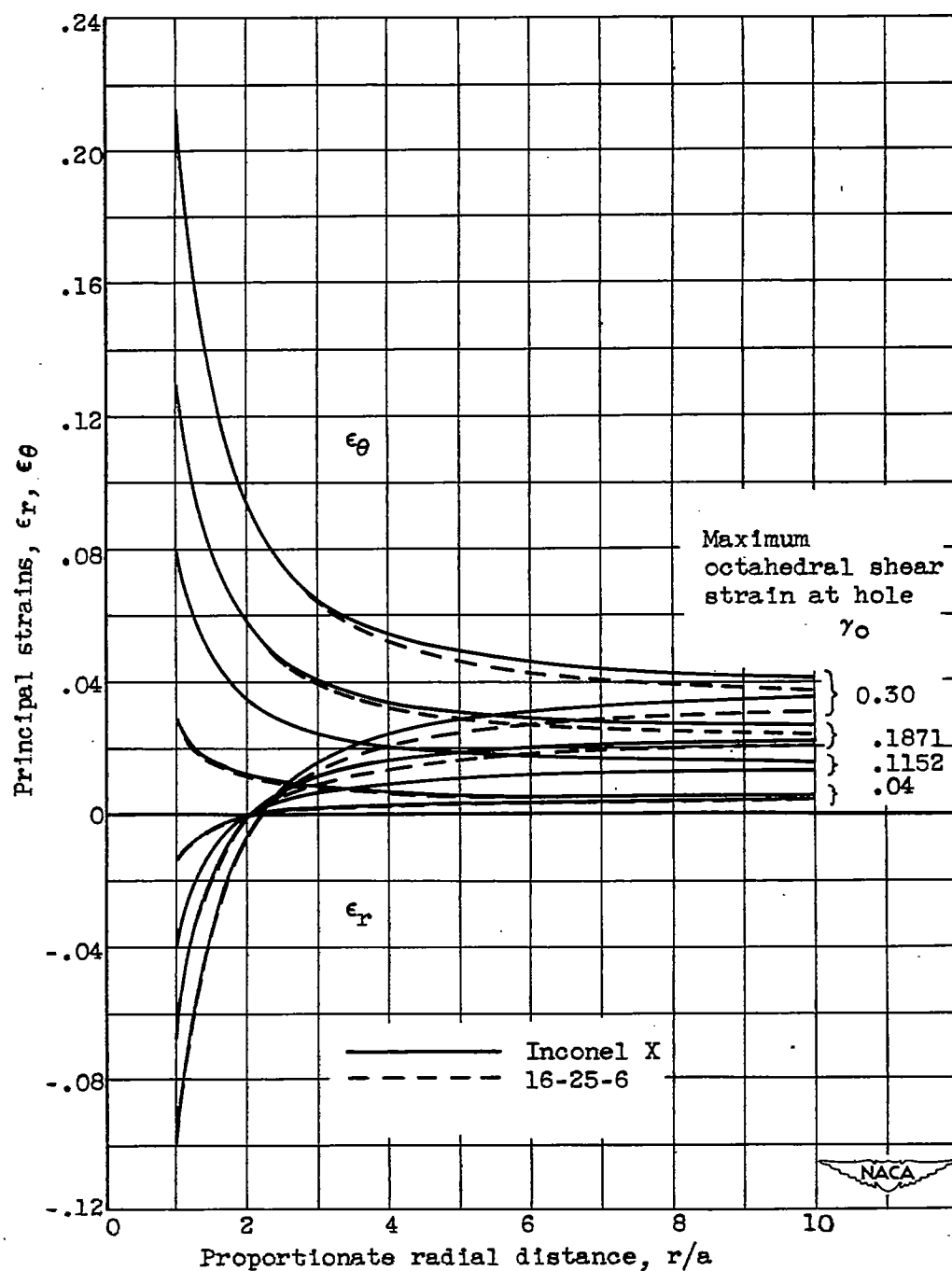
(b) Infinite plate with hole.

Figure 14. - Concluded. Variation of principal stresses σ_r and σ_θ with proportionate radial distance.



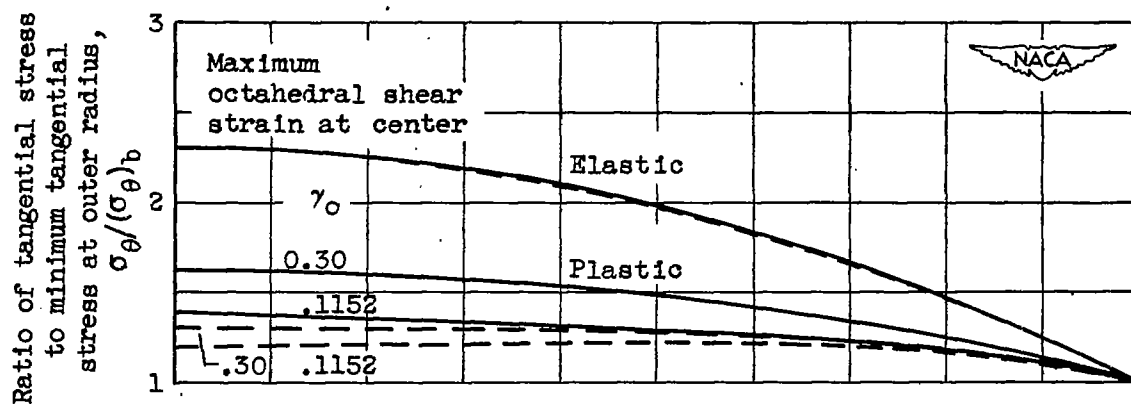
(a) Rotating disk.

Figure 15. - Variation of radial and circumferential strains ϵ_r and ϵ_θ with proportionate radial distance.

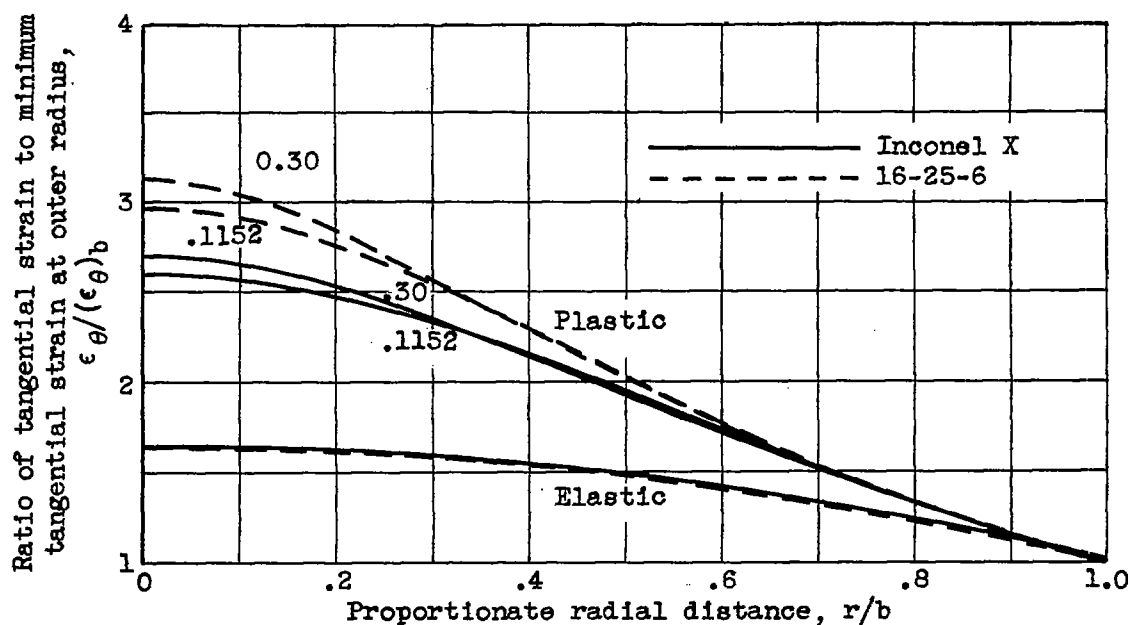


(b) Infinite plate with holes.

Figure 15. - Concluded. Variation of radial and circumferential strain ϵ_r and ϵ_θ with proportionate radial distance.

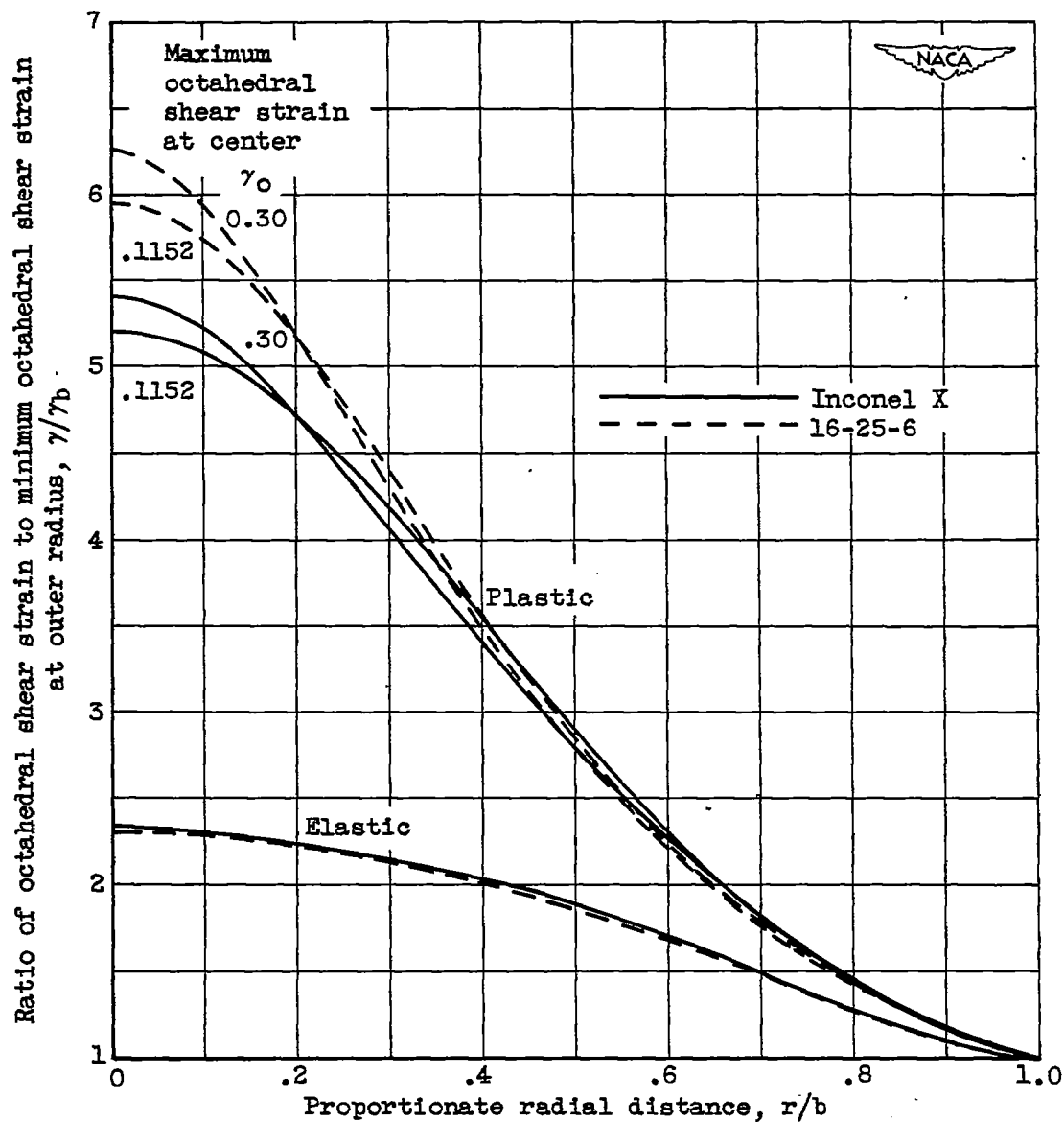


(a) Variation of ratio of tangential stress to minimum tangential stress at outer radius with proportionate radial distance.



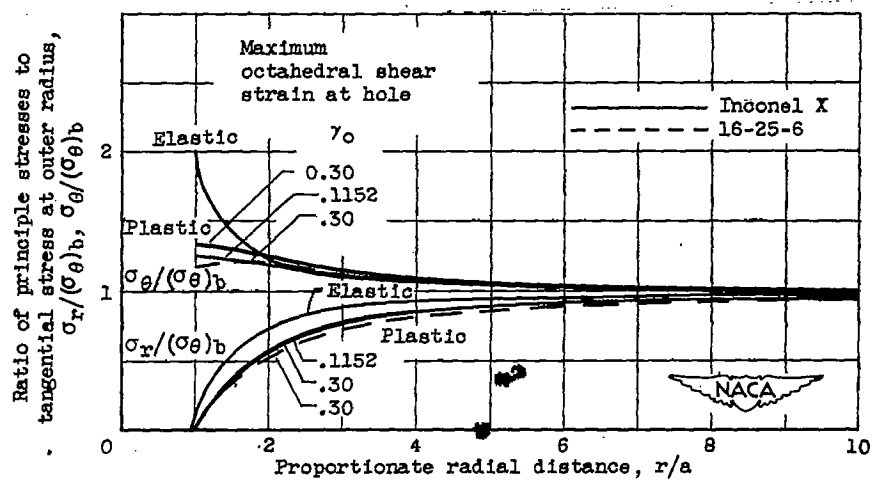
(b) Variation of ratio of tangential strain to minimum tangential strain at outer radius with proportionate radial distance.

Figure 16. - Comparison of results obtained in elastic and plastic range for rotating disk.



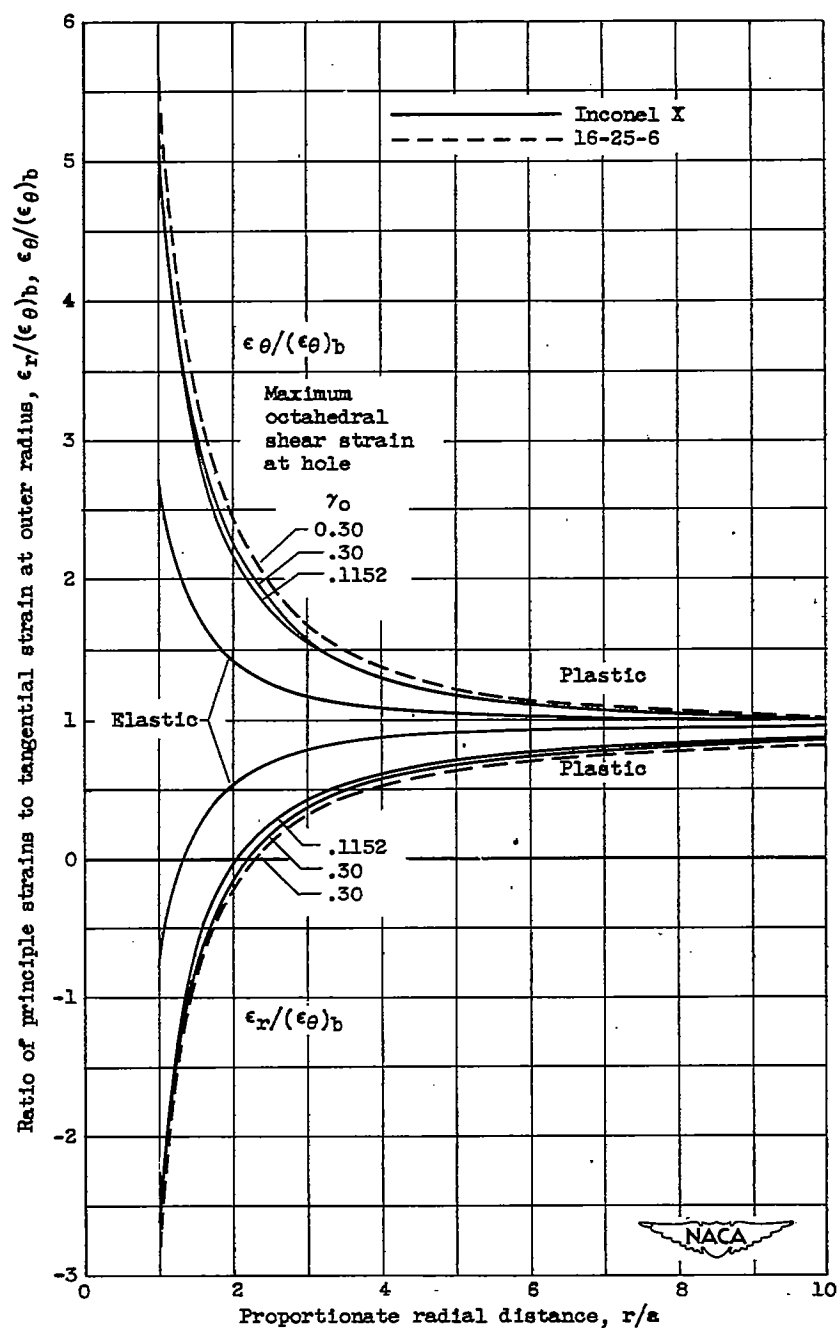
(c) Variation of ratio of octahedral shear strain to minimum octahedral shear strain at outer radius with proportionate radial distance.

Figure 16. - Concluded. Comparison of results obtained in elastic and plastic range for rotating disk.



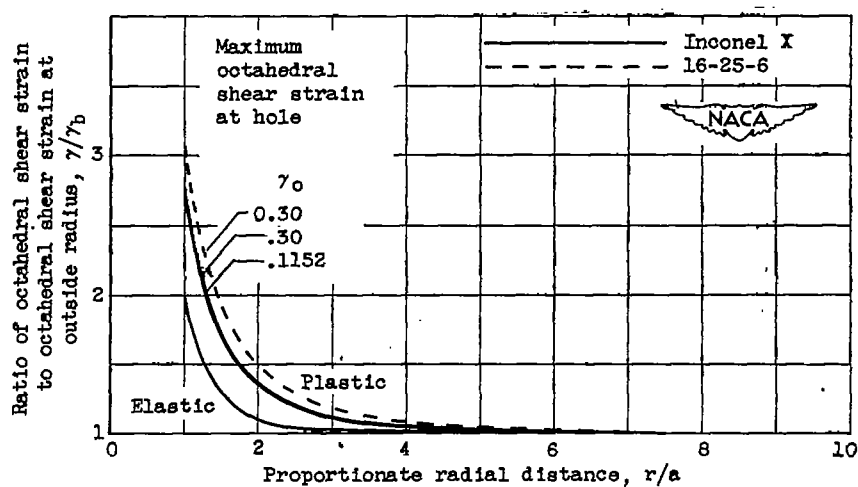
(a) Variation of ratio of principal stresses to tangential stress at outer radius with proportionate radial distance.

Figure 17. - Comparison of results obtained in elastic and plastic range for infinite plate with circular hole.



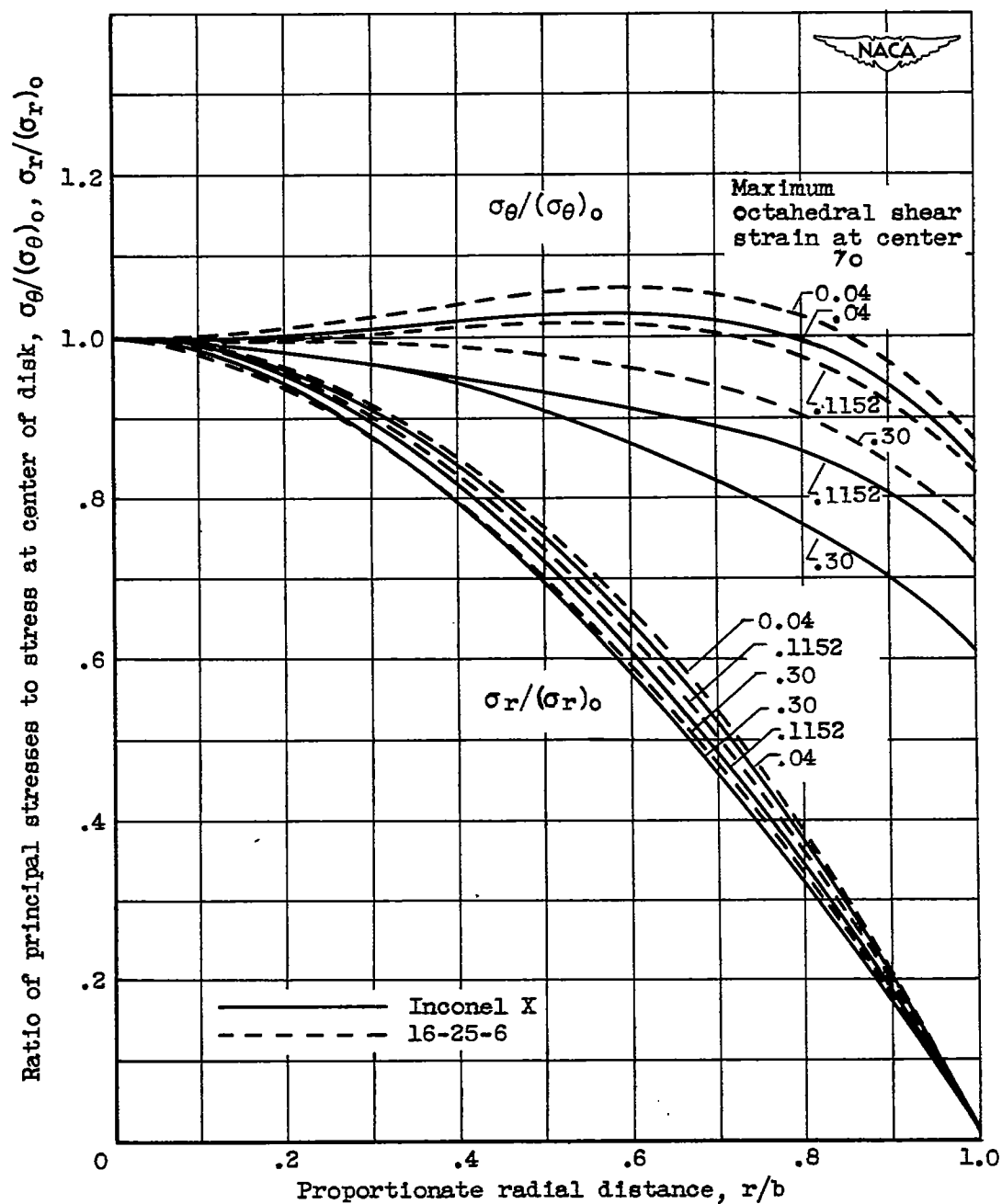
(b) Variation of ratio of principal strains to tangential strain at outer radius with proportionate radial distance.

Figure 17. - Continued. Comparison of results obtained in elastic and plastic range for infinite plate with circular hole.



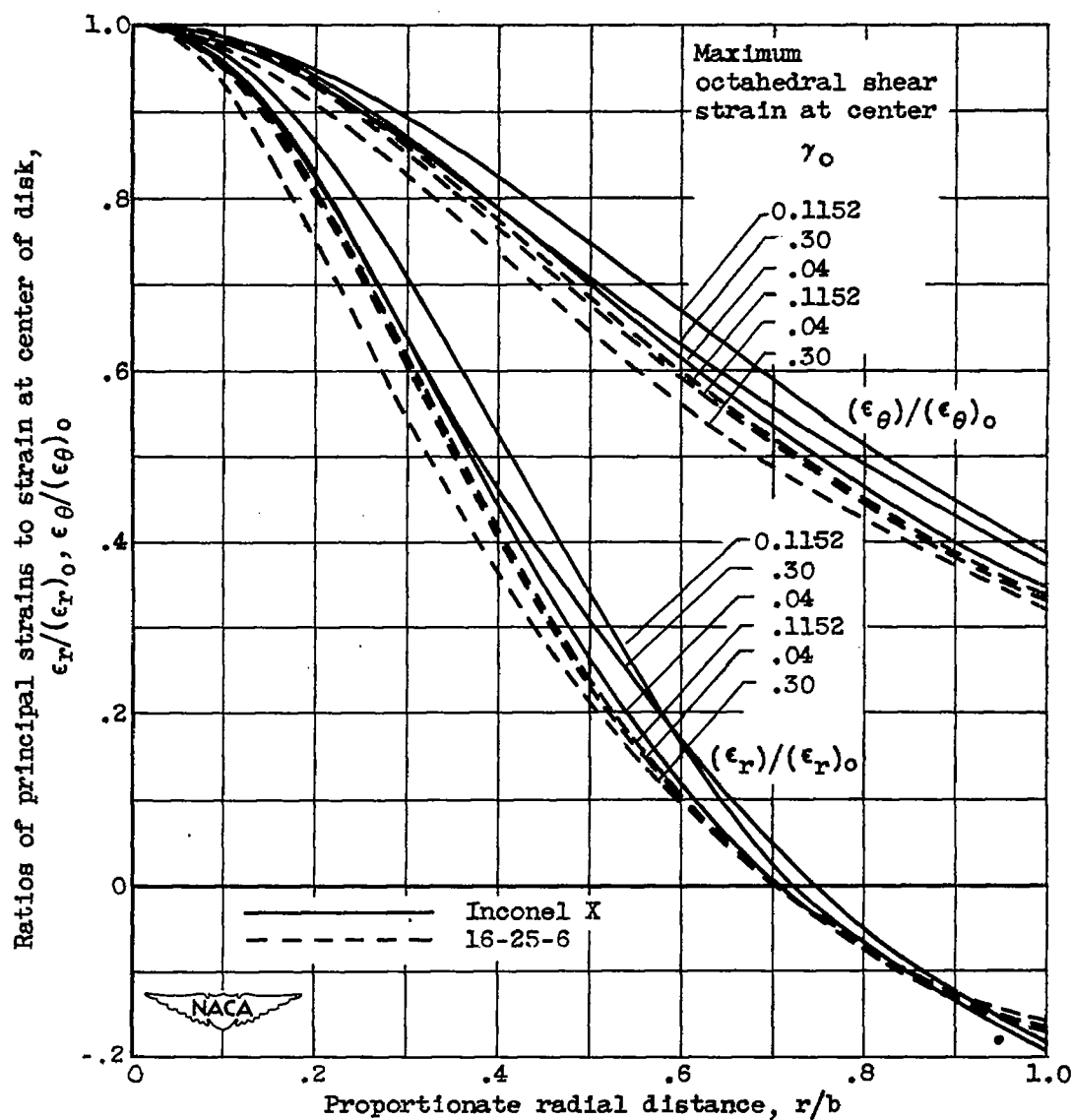
(c) Variation of ratio of octahedral shear strain to octahedral shear strain at outer radius with proportionate radial distance.

Figure 17. - Concluded. Comparison of results obtained in elastic and plastic range for infinite plate with circular hole.



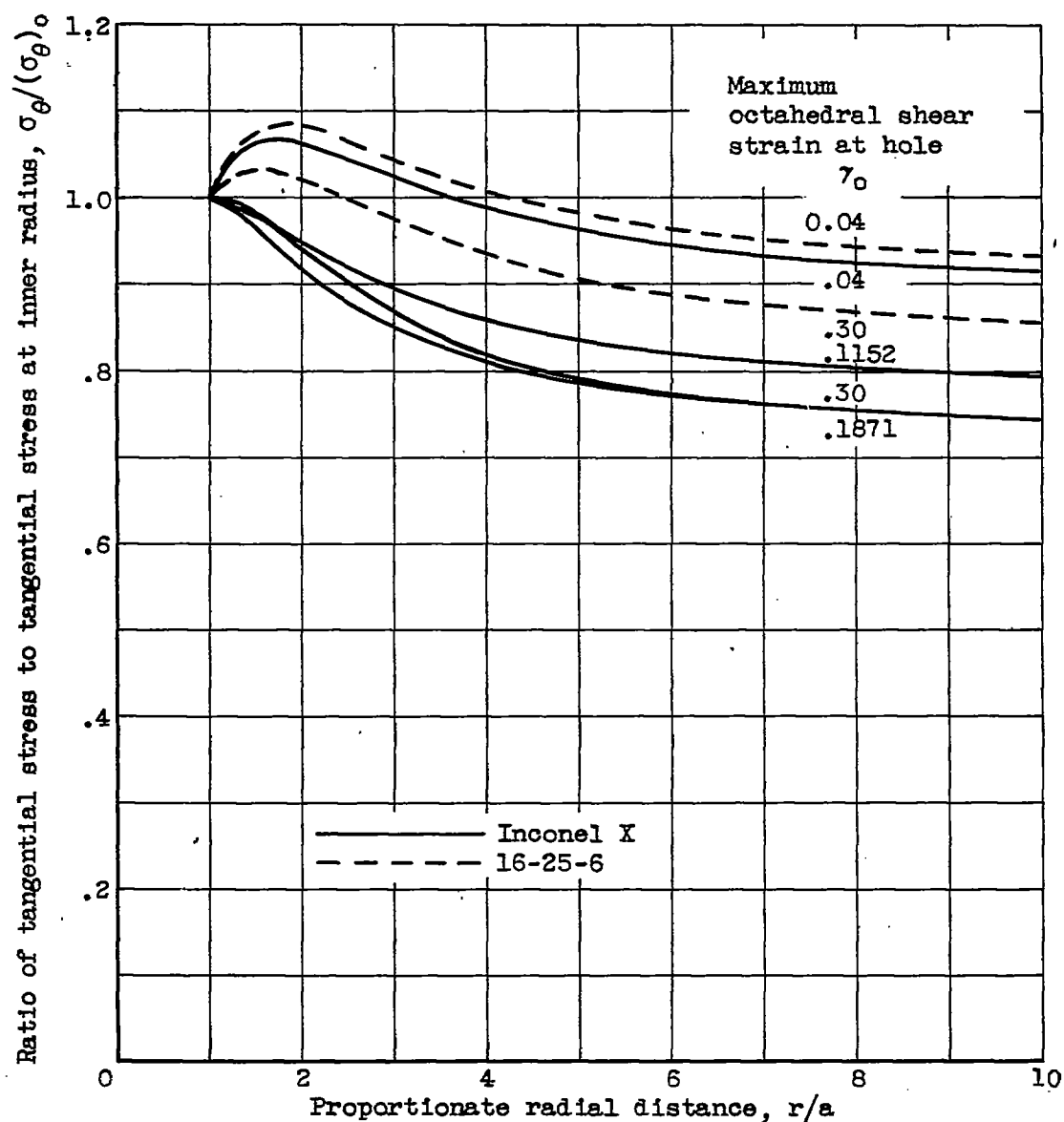
(a) Variation of ratio of principal stresses to stress at center of disk with proportionate radial distance.

Figure 18. - Comparison of stress and strain distributions for different materials and for different maximum octahedral shear strain of rotating disk.



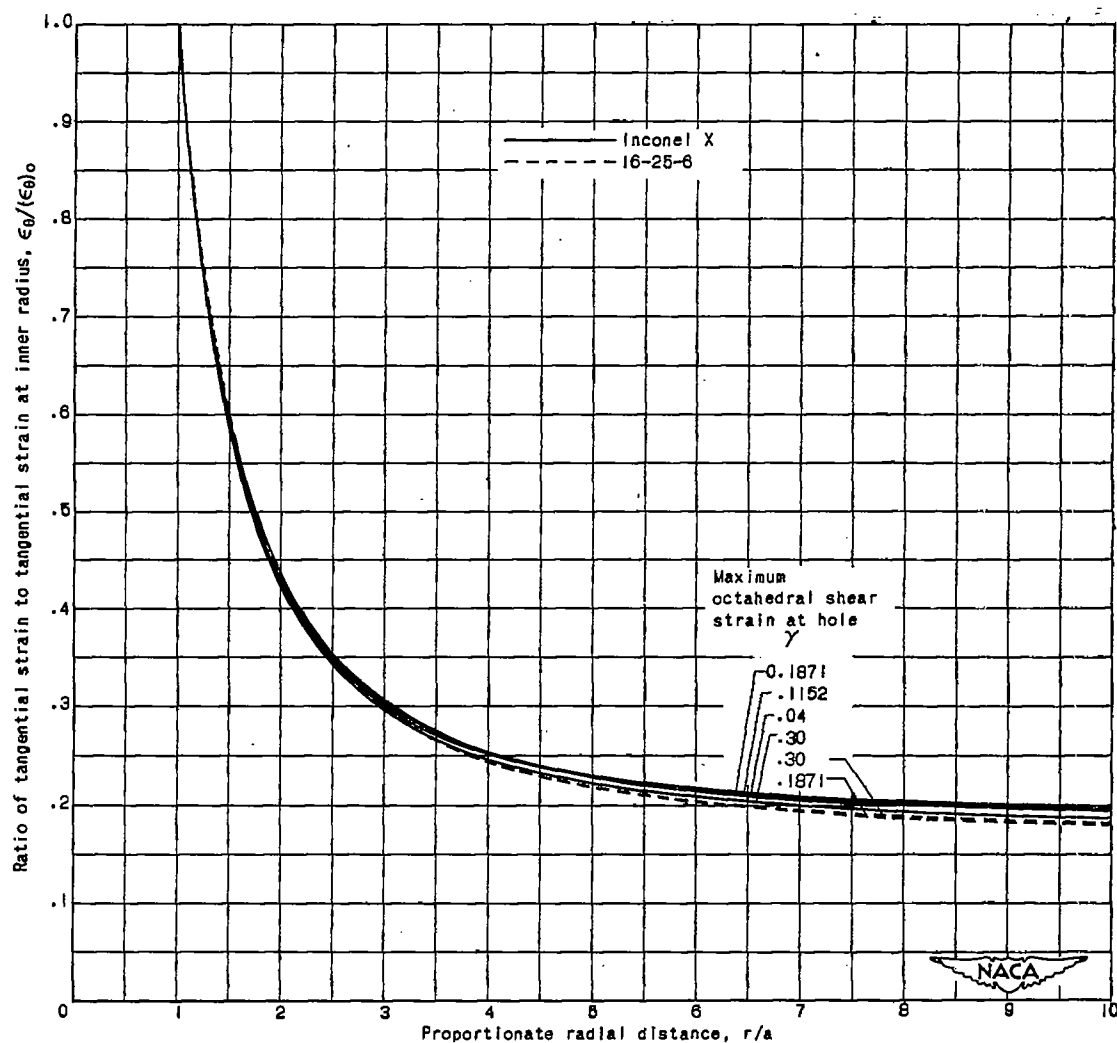
(b) Variation of ratios of principal strains to strain at center of disk with proportionate radial distance.

Figure 18. - Concluded. Comparison of stress and strain distributions for different materials and for different maximum octahedral shear strain of rotating disk.



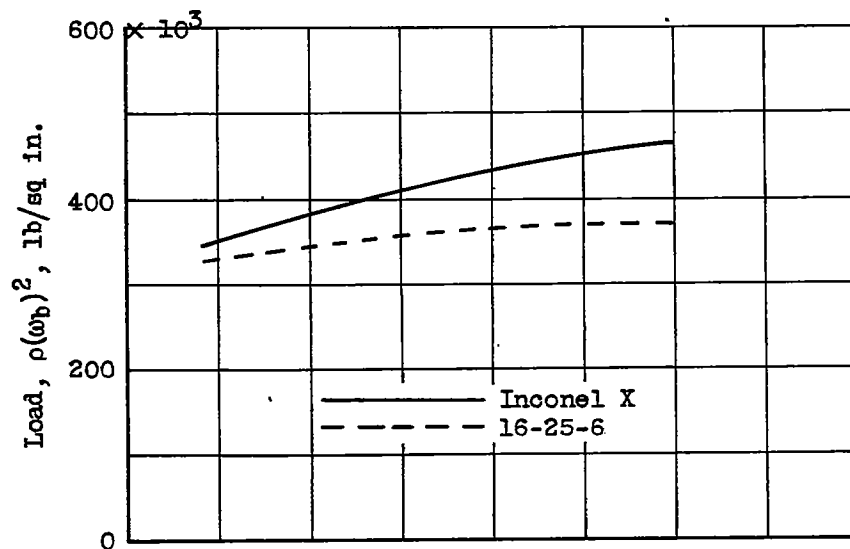
(a) Variation of ratio of tangential stress to tangential stress at inner radius with proportionate radial distance.

Figure 19. - Comparison of stress and strain distributions for different materials and for different maximum octahedral shear strain of infinite plate with circular hole.

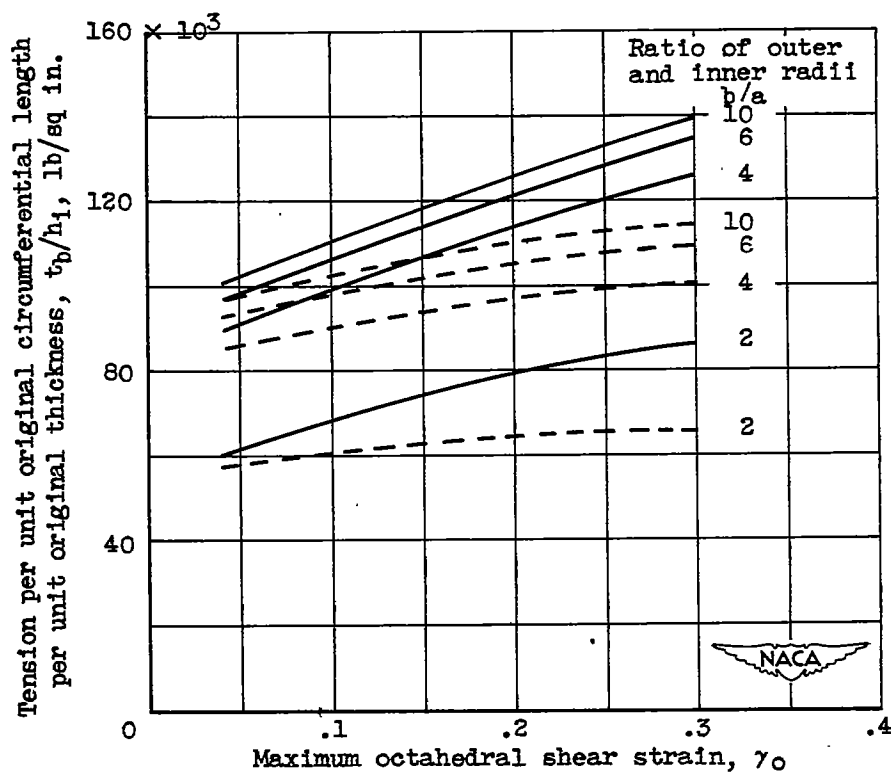


(b) Variation of ratio of tangential strain to tangential strain at inner radius with proportionate radial distance.

Figure 19. - Concluded. Comparison of stress and strain distributions for different materials and for different maximum octahedral shear strain of infinite plate with circular hole.

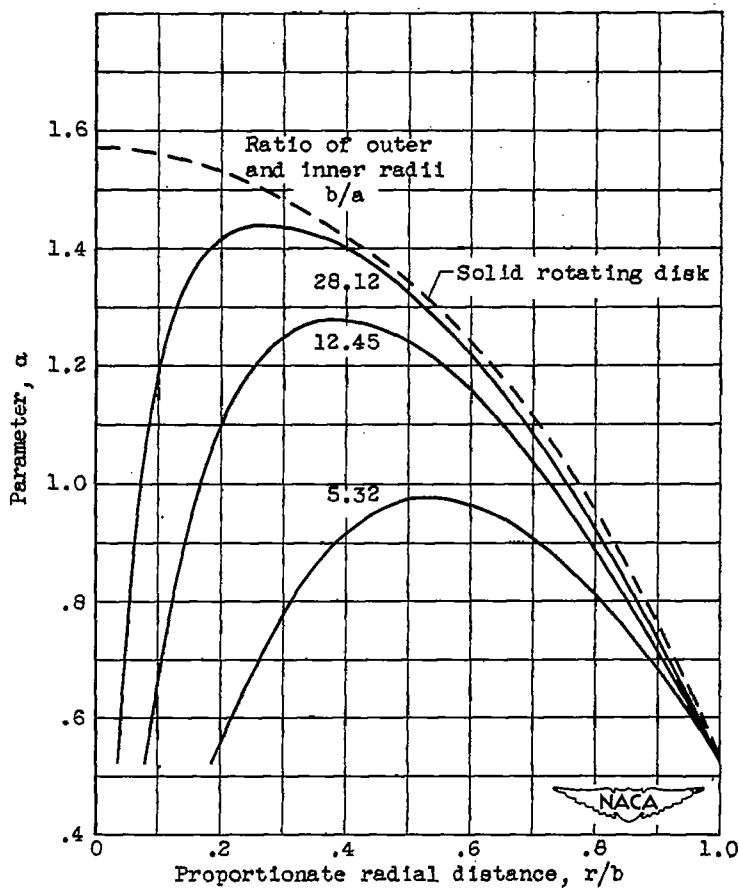


(a) Solid rotating disk.



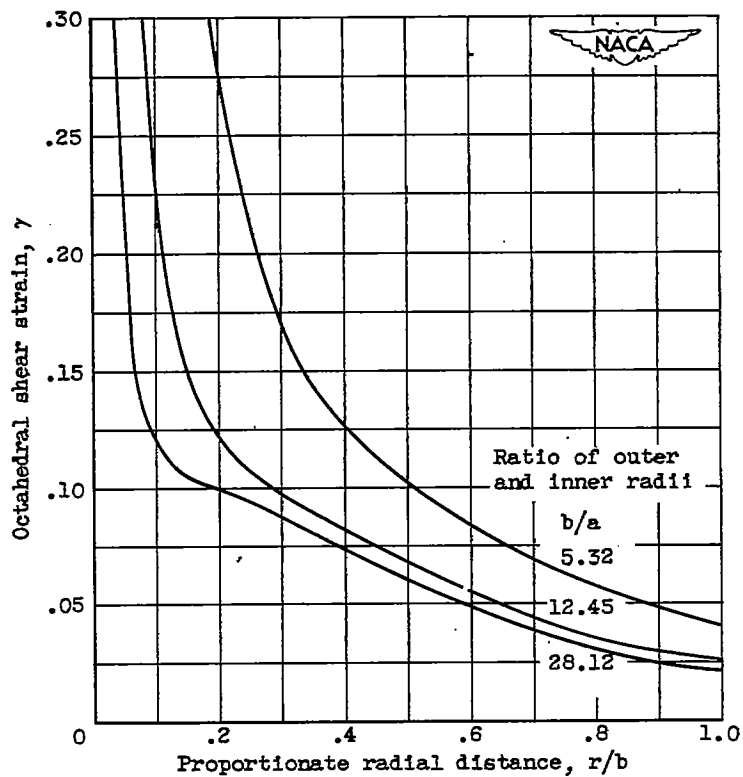
(b) Flat ring radially stressed.

Figure 20. - Relation between load and maximum octahedral shear strain.



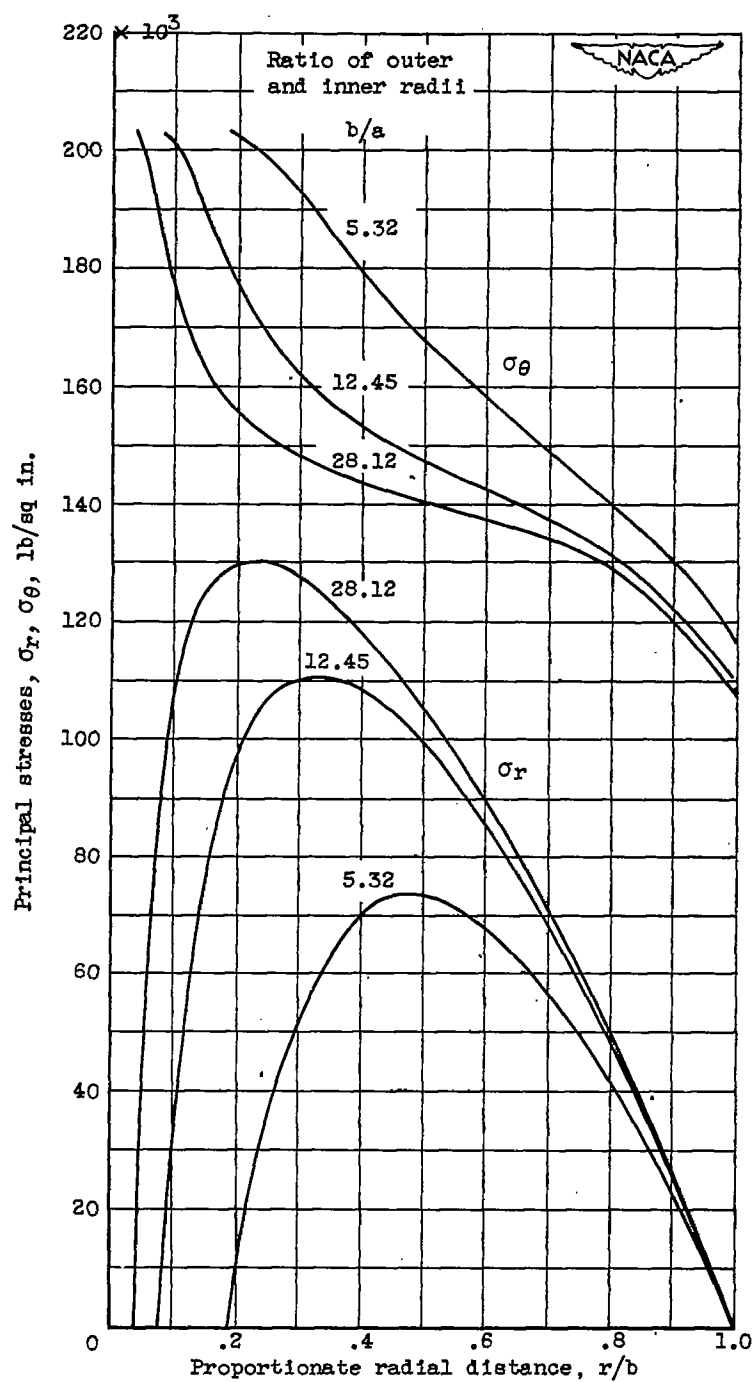
(a) Variation of parameter α with proportionate radial distance.

Figure 21. - Rotating disk with hole, Inconel X, $\gamma_0 = 0.30$.



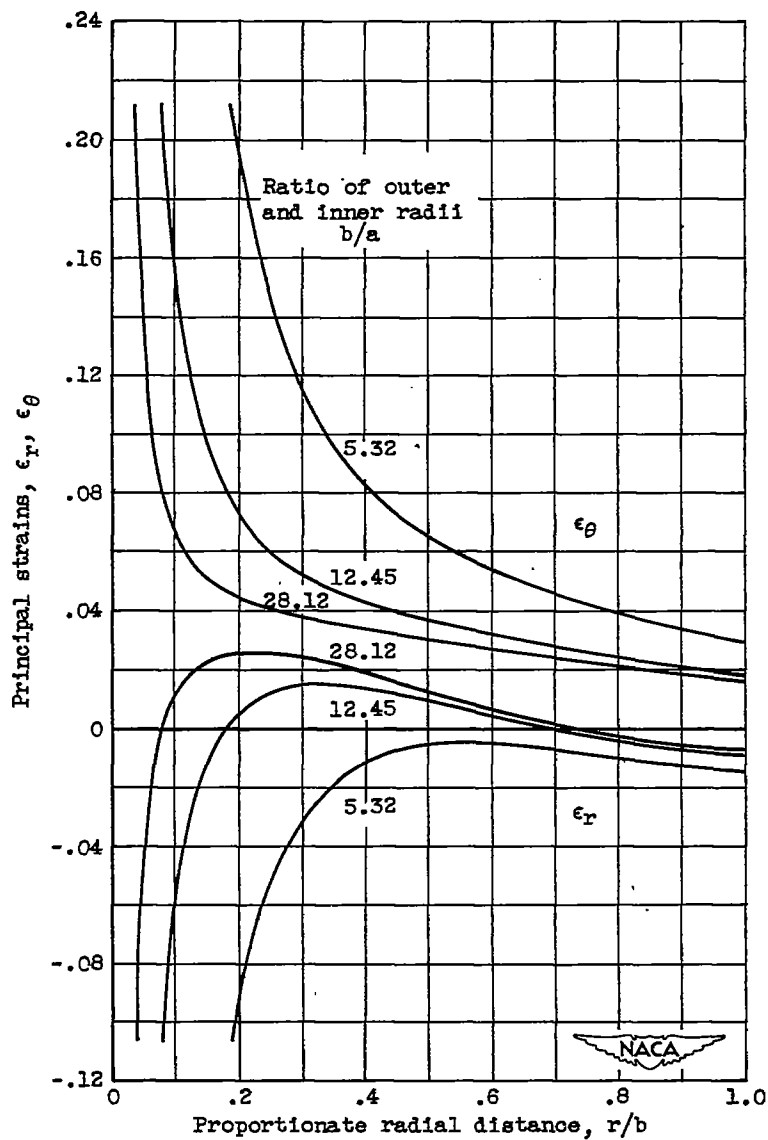
(b) Variation of octahedral shear strain with proportionate radial distance.

Figure 21. - Continued. Rotating disk with hole, Inconel X, $\gamma_0 = 0.30$.



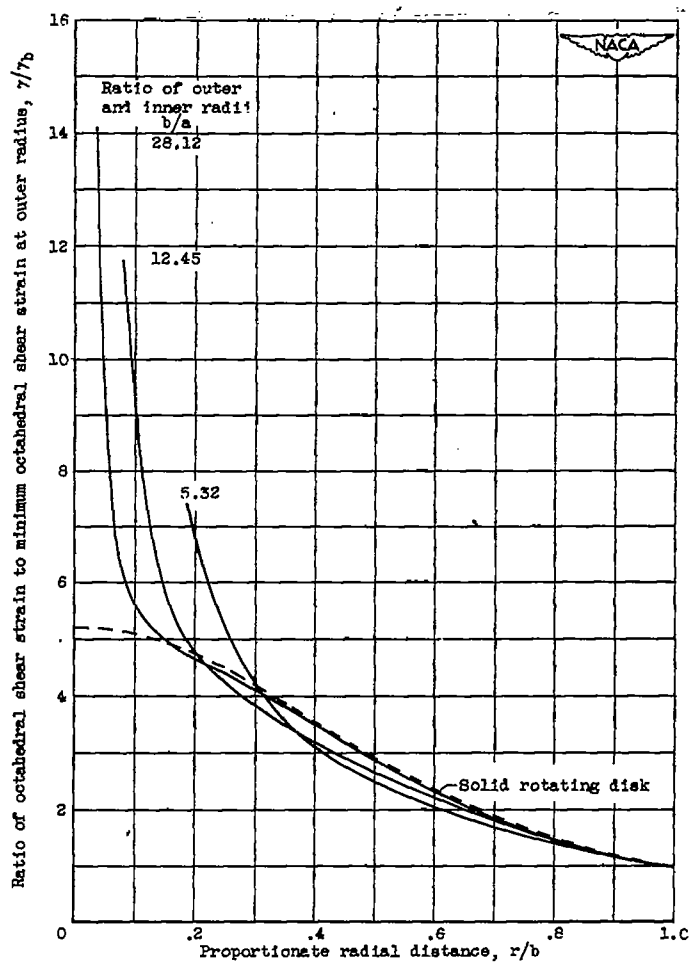
(c) Variation of principal stresses with proportionate radial distance.

Figure 21. - Continued. Rotating disk with hole, Inconel X, $\gamma_0 = 0.30$.



(d) Variation of principal strains with proportionate radial distance.

Figure 21. - Continued. Rotating disk with hole, Inconel X, $\gamma_0 = 0.30$.



(e) Variation of ratio of octahedral shear strain to minimum octahedral shear strain at outer radius with proportionate radial distance.

Figure 21. - Concluded. Rotating disk with hole, Inconel X, $\gamma_0 = 0.30$.

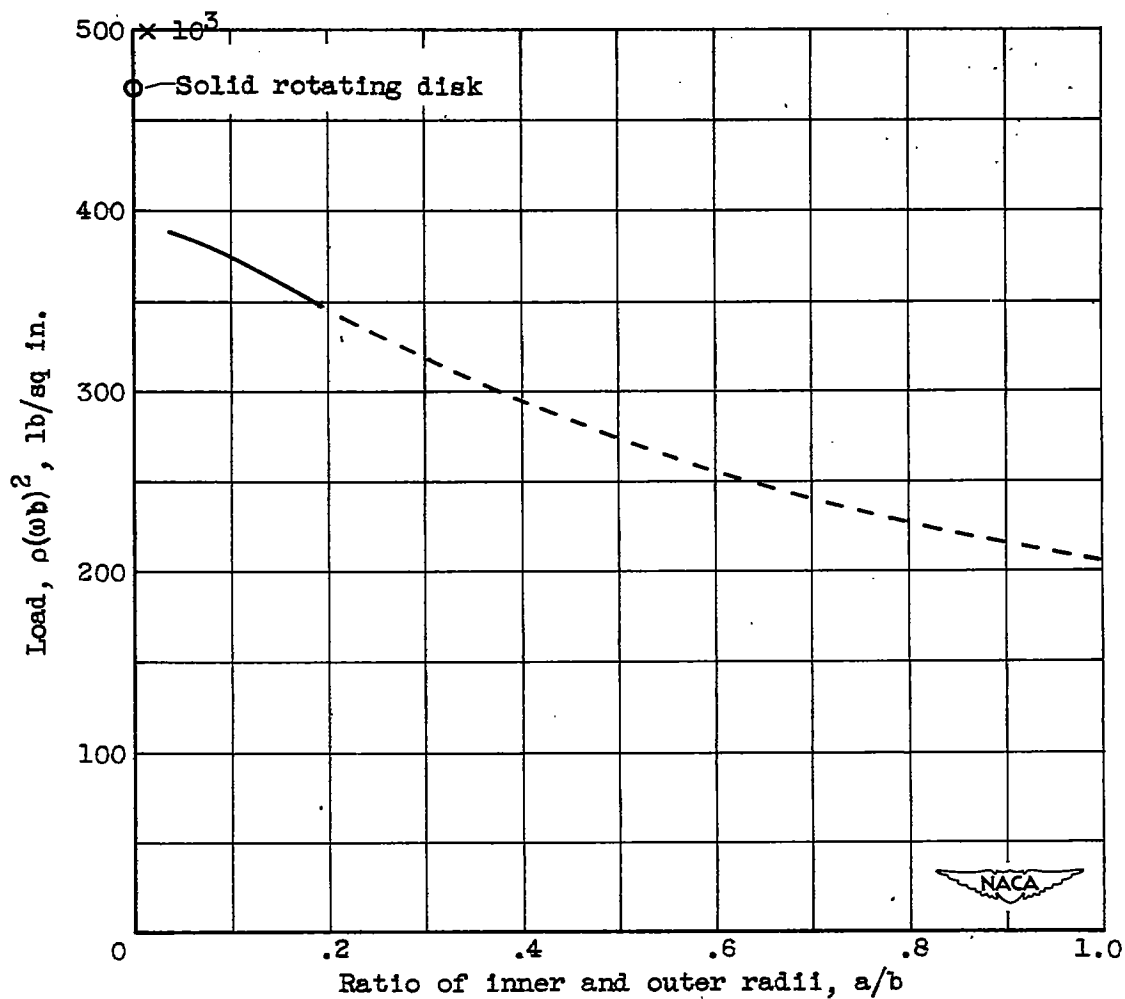


Figure 22. - Variation of load (function of speed) with ratio of inside and outside radii of rotating disk with hole. Inconel X; $\gamma_0 = 0.3$.